

~

## Chapter Three

# The hydrogen fuel cell power system

~

This chapter discusses two major issues: (i) fuel cell theory and engineering, and (ii) providing fuel for the fuel cell.

The first section thoroughly discusses the science behind fuel cells in general. Of the different kinds of fuel cells, the proton exchange membrane type is identified as the unquestioned best candidate for the small vehicle application. Engineering issues like how to cool the fuel cell stack and whether to pressurize the fuel cell are discussed in general terms and the feasibility of certain design options is determined. (On the other hand, more complete, quantitative analyses of cooling and pressurization require more detailed information about steady-state and transient power requirements that are not calculated until Chapter 4, and are thus properly analyzed within that chapter). The size and weight of the fuel cell are discussed with reference to previous researchers' results.

The second half of this chapter concerns fueling of hydrogen fuel cells, which is considerably more complex than filling a tank with gasoline. It explains why reformed fossil fuels cannot yet be used to power a fuel cell vehicle, and describes various options for storing pure hydrogen on board the vehicle. The issue of safety is discussed.

## 3.1. Fuel Cell Science

---

### 3.1.1. Fundamentals

Fuel cells are electrochemical engines that produce electricity from paired oxidation / reduction reactions. One can think of them as batteries with flows of reactants in and products out. In contrast, the battery has a fixed supply of reactants that transform into products without being steadily replaced. The distinction is a nice one as zinc-air “batteries” have replaceable zinc electrodes, making them very like fuel cells.

A standard high school chemistry demonstration involves passing an electric current from a battery through a jar of water (with dissolved salts) by way of two metal electrodes suspended in the water. Hydrogen evolves at the cathode and oxygen at the anode as the water is broken into its constituent elements by electrolysis. Essentially, a fuel cell uses the reverse process: hydrogen and oxygen are combined to form water, and electricity is produced.

Technically, the two chemicals do not have to be hydrogen and oxygen; the redox reaction requires only a reducer and an oxidizer, but since oxygen is easy to obtain from the air and hydrogen has suitably fast reaction kinetics, these are the two most often chosen. All further examples will use hydrogen and oxygen unless otherwise noted.

Specifically, the hydrogen and oxygen diffuse into their respective electrodes, ionize, and one type of ion migrates through an electrolyte and recombines at the other side with the other ion to form water. At any given temperature there is an equilibrium ratio of ions to molecules. Coatings of

noble metal catalyst on the electrodes lower the activation energy of the ionization / recombination process, accelerating the restoration of equilibrium as the ions are consumed by the fuel cell.

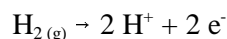
The principle behind fuel cells was discovered as early as 1839 by Welsh physicist and judge Sir William Grove. However, due to high costs, the technology was not significantly used until the American Gemini space missions of the 1960's. For this and subsequent space missions, fuel cells were thought to be safer than nuclear electric generation and cheaper than solar. They have been thrust to the forefront of energy technology in the 1990's, however, as high power densities have made them feasible for both stationary and portable applications. ONSI corporation, a subsidiary of United Technologies, has produced over 170 of its PC25 stationary 200 kW fuel cell systems since their introduction in 1992.

Fuel cells have the advantages of high efficiency, low or even zero pollution, quiet operation, and fewer moving parts – only pumps and fans to circulate coolant and reactant gases, respectively – for greater reliability than internal combustion engines (once fuel cell systems are well-developed).

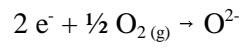
### *3.1.1.1 Thermodynamics*

An electrolyte physically separates the two reactants and also prevents electronic conduction, while allowing ions to pass through; the electrons travel through an external loop to supply the load.

Electrodes are attached to either side of the electrolyte. At the anode, the hydrogen is oxidized:



The electrons pass through the load to provide the desired current and end up at the cathode, where the matching reduction reaction occurs:



Electrostatic balance is reached as the hydrogen ions diffuse through the electrolyte to get to the cathode:

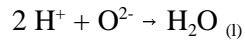
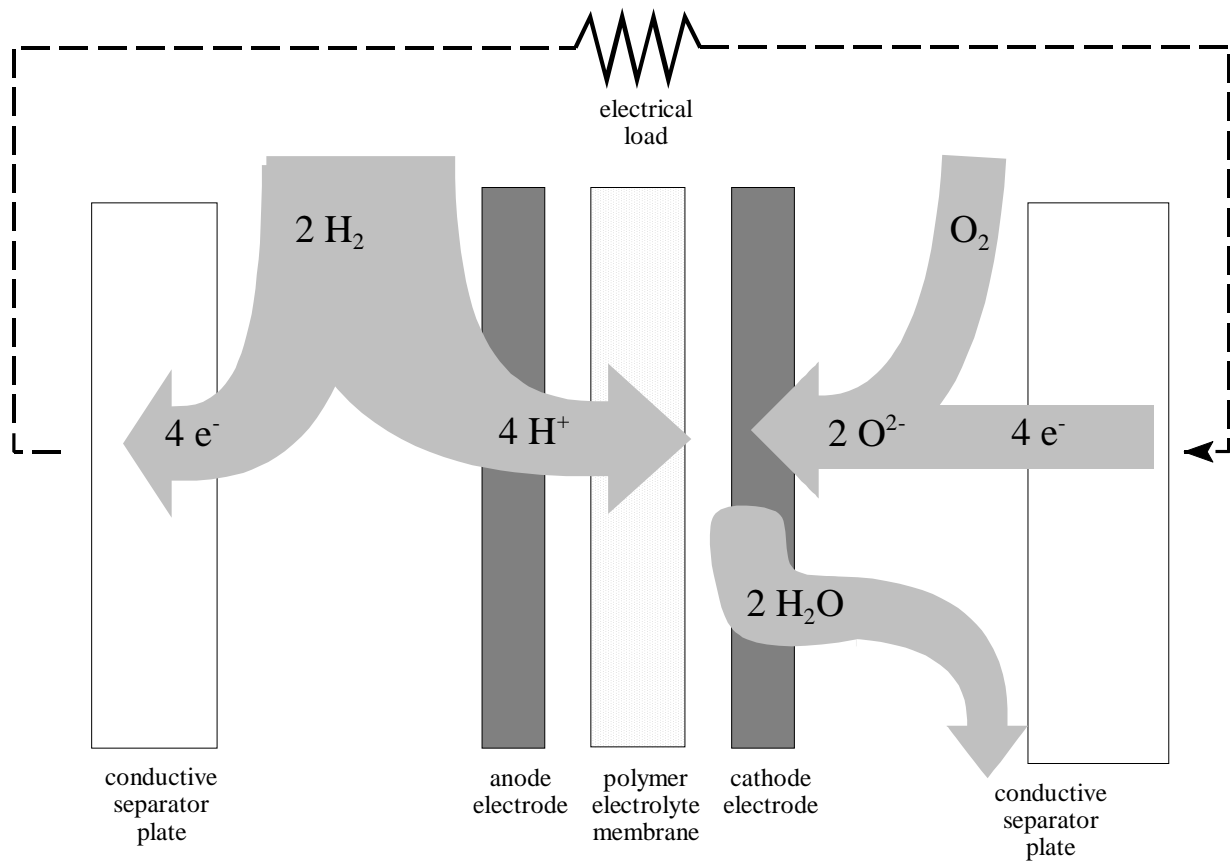
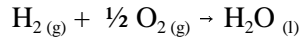


*Figure 3.1 Fuel cell schematic*



The theoretical energy release of the overall reaction is determined by the enthalpy change  $\Delta H$  in the overall (isothermal) reaction,



$$(\Delta H^\circ = -285.8 \text{ kJ/mol}; \Delta G^\circ = -237.2 \text{ kJ/mol}; )$$

$\Delta G$  is the Gibbs free energy and standard conditions, as indicated by the nought superscript, are  $T=25^\circ\text{C}$ , partial pressures of 1 atm for each of the gases, and water in the liquid state. This last distinction is important. For high temperature fuel cells, water emerges in the gaseous state, so the “lower heating value” would be used. In this (non-standard) case,  $\Delta H = -241.8 \text{ kJ/mol}$  and  $\Delta G = -228.6 \text{ kJ/mol}$ . The higher heating value is used in the remaining calculations since most fuel cells operate below the boiling point of water.

The next step is to determine fuel cell efficiency.

$$\Delta G^\circ = \Delta H^\circ - T\Delta S^\circ$$

so the standard change in entropy is  $-0.163 \text{ kJ} \cdot \text{mol}^{-1} \cdot \text{K}^{-1}$ . An energy balance on a fuel cell shows that

$$d/dt (dQ + dW_{\text{elec}}) = d/dt (dH + dKE + dPE)$$

Kinetic energy (KE) and potential energy (PE) changes are assumed to be negligible, and steady state operation is assumed. A “perfect” fuel cell operating irreversibly means  $dQ = T dS$ . Thus,  $W_{\text{elec}}$ , the electrical power output, is

$$W_{\text{elec}} = \Delta H - T\Delta S = \Delta G$$

Efficiency at any given point is usually defined here by dividing the maximum work out by the enthalpy input, so fuel cell efficiency is:

$$\eta_{FC} = \Delta G / \Delta H$$

Using the standard free energy and enthalpy given previously ( $\Delta G^\circ = -237.2$  kJ/mol,  $\Delta H^\circ = -285.8$  kJ/mol) shows the maximum thermodynamic efficiency under standard conditions is 83%.

The change in standard free energy can be used to calculate the maximum reversible voltage provided by the cell:

$$\Delta G^\circ = -nFE_r^\circ$$

where  $n$  is the number of electrons in the reaction as written,  $F$  is Faraday's constant (96,487 coulombs per mole of electrons), and  $E_r^\circ$  is the *standard* reversible potential. Since  $n=2$  here,  $E_r^\circ = 1.229$  V. This reversible potential changes with changing pressure as the Nernst equation:

$$E_r = E_r^\circ + \frac{RT}{nF} \ln \left( \frac{A_{H_2} A_{O_2}^{1/2}}{A_{H_2O}} \right)$$

Again,  $n=2$ , and the "A"s are the activities of the various species – the partial pressures for hydrogen and oxygen, and 1 for water since it is in the liquid form. (Activity measures the concentration relative to standard conditions, so for the gases this becomes the partial pressure relative to 1 atm, and for solutes it is relative to a 1-molality solution in solvent. Water *is* the solvent, so its activity is 1) The voltage increase derived from an increase in pressure by a factor  $\lambda$  (assuming that the hydrogen intake pressure is increased by the same factor as the oxygen intake), is given below.

$$\Delta E_r = \frac{RT}{nF} \ln \left( \frac{P_{H_2(2)}^* P_{O_2(2)}^{*1/2}}{P_{H_2(1)}^* P_{O_2(1)}^{*1/2}} \right) = \frac{RT}{nF} \ln \lambda^{1.5} = 1.5 \frac{RT}{nF} \ln \lambda$$

The “(2)” subscripts refer to the pressurized states of the reactant gases and the “(1)” to the unpressurized partial pressures. At 80°C and 2 moles of electrons in the reaction as written, the theoretical voltage change is 16 mV for a doubling of the intake pressures from the default 1 atm to 2 atm. For an increase in pressure to 300 kPa, a typical figure used for fuel cells, a voltage increase of 25 mV could be realized. However, as the next section on kinetics shows, the improvement  $\Delta E_r$  is actually much larger.

(Some researchers have considered variable-pressure systems where greater compression is used when higher power is demanded. This produces higher efficiencies at high power, and lower parasitic compressor losses at low power. On the other hand, a constant-pressure fuel cell is cheaper and simpler to manufacture.)

The relationship between voltage and temperature is derived by taking the free energy, linearizing about the standard condition of 25°C, and assuming that the enthalpy change  $\Delta H$  does not change with temperature:

$$E_r = -\frac{\Delta G}{nF} = -\frac{\Delta H - T\Delta S}{nF}$$

$$\Delta E_r = \left. \frac{dE_r}{dT} \right|_p \Delta T$$

$$\Delta E_r = \left. \frac{dE_r}{dT} \right|_p (T - 25^\circ C) = \frac{\Delta S}{nF} (T - 25^\circ C)$$



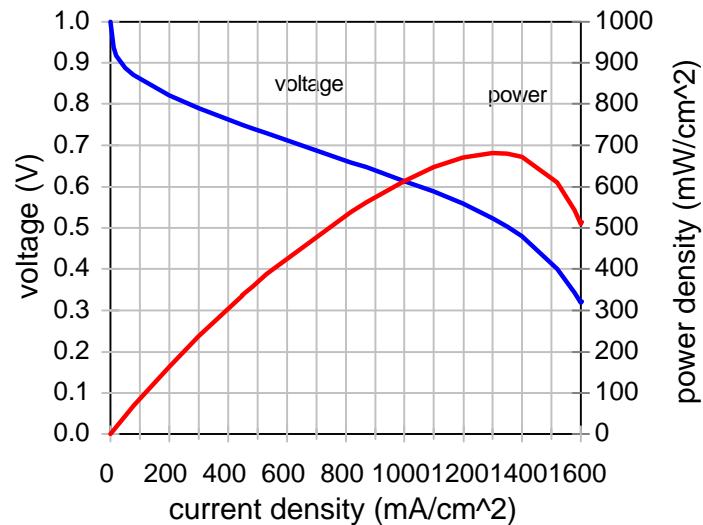
Because the change in entropy is negative, the open-circuit voltage output decreases with increasing temperature; the fuel cell is theoretically more efficient at low temperatures. However, other effects like mass transport and ionic conduction are faster at higher temperatures and this more than offsets the drop in open-circuit voltage.

In theory, the power generated by a single fuel cell is simply the reversible potential times the number of electrons generated per second (i.e. the current). The fuel cells are connected in a “stack” to multiply the power.

#### *3.1.1.2 Kinetics*

The cell potential, however, is also limited by the kinetics of the reaction. These losses are most often shown in what is known as a Tafel plot or polarization curve; cell potential in volts is graphed against the cell current density in amperes per square centimeter of cell area. The current density basically represents how fast the reaction is taking place (it is the number of electrons per second, divided by the surface area of the fuel cell electrolyte face); measured voltage divided by reversible voltage is equal to the efficiency defined previously. The power curve as a function of current ( $V \cdot i$  versus  $i$ ) shows a peak at high current density.

**Figure 3.2 Tafel plot**



At non-zero current densities, there is what is known as an “activation overpotential”: to drive the dissociation of the oxygen and hydrogen molecules quickly, a certain activation energy must be exceeded. Essentially, the oxygen and hydrogen molecules must diffuse in through pores in the metal catalyst and adsorb. This is a “three phase interface problem,” since gaseous fuel, solid metal catalyst, and liquid electrolyte must all contact. The catalyst reduces the height of the activation barrier but a loss in voltage remains due to the still-slow oxygen reaction. (Note that the hydrogen activation overpotential is negligible compared to the oxygen overpotential; the oxygen reaction is five to six orders of magnitude slower.<sup>1</sup>) Also, competing reactions occur at the oxygen electrode: oxidation of the platinum, corrosion of carbon support, and oxidation of organic impurities on the electrode. The total overpotential is 0.1 to 0.2 V, reducing the maximum potential to less than 1.0 V even under open-circuit conditions.<sup>2</sup>

There is also a continuous drop in voltage as current increases, and this is due to linear, ohmic losses (i.e. resistance) in the ionic conduction through the electrolyte. The thinner the membrane,

the lower this loss. Thinner membranes are also advantageous because they keep the anode electrode wet by “back” diffusion of water from the cathode, where it is generated, towards the anode.

Finally, at very high current densities (fast fluid flows), mass transport causes a rapid drop-off in the voltage, because oxygen and hydrogen simply cannot diffuse through the electrode and ionize fast enough, and products cannot be moved out quickly enough.

The Tafel plot is often modeled semi-empirically with an equation of the form

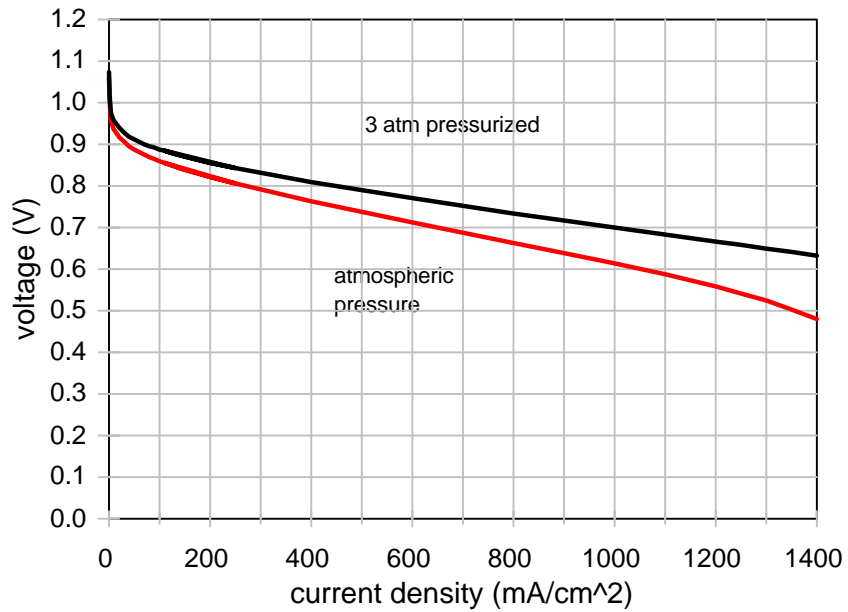
$$E = E_o - b \ln(i) - Ri - m e^{ni}$$

where the voltage  $E$  is a function of current density  $i$ .

Higher pressure improves kinetics as well as thermodynamics due to the higher concentration of reactants; the Nernst equation does not tell the whole story. For an increase in pressure to 300 kPa, a voltage increase of 25 mV is expected from the Nernst equation. The additional voltage derived from the kinetics of the reaction is estimated at 29 mV for 3 atm operation by one researcher.<sup>3</sup> This doubles the voltage increase to 54 mV. The gain in voltage in a Ballard Mk IV single cell operating at 400 mA•cm<sup>2</sup> was experimentally determined to be 2.7 times greater than predicted by the Nernst equation for - in the example of pressurizing to 3 atm, this is an increase of 67.5 mV.<sup>4</sup>

In terms of the overall effect of pressurization, significantly larger increases in voltage are often realized at 300 kPa, as the following Energy Partners polarization curves below show. Here, the difference in voltages widens to as much as 0.150 V (25%) at 1400 mA•cm<sup>2</sup>. At 1000 mA•cm<sup>2</sup>, the improvement is 14%.

*Figure 3.3 Effects of pressurization on polarization curves*



Data from Barbir is for a single cell running on hydrogen/air, with a Gore MEA and operating temperature of 60°C. Air-side stoichiometry is 2.5, meaning that 2.5 times as much oxygen is supplied than the minimum needed for stoichiometry.<sup>5</sup>

### *3.1.1.3 A note on efficiency*

Since efficiency will later be used to calculate waste heat generation, the method here is to divide electrical power output by the rate of energy consumed. As alluded to earlier, “energy consumed” is measured in terms of the higher heating value of the hydrogen used.

In other words,

$$\text{Efficiency } \eta = \frac{\text{power}_{out}}{\text{power}_{in}} = \frac{\dot{n}_{electrons} F V_{output}}{\dot{n}_{hydrogen} \Delta H_{HHV}} = \frac{2 F V_{output}}{\Delta H_{HHV}}$$

where  $\dot{n}$  are flow rates in moles per second, F is the Faraday constant, V is the voltage of the cell output, and  $\Delta H_{HHV}$  is -285.8 kJ/mol. In practice, the higher heating value enthalpy can be converted to an equivalent voltage of 1.481 V, so that

$$\eta = \frac{V_{output}}{1.481V}$$

This equivalent voltage concept is very useful in calculating efficiency and waste heat; with the efficiency defined in this way, the waste heat generated is simply

$$\dot{Q} = \dot{n} \Delta H_{HHV} (1 - \eta)$$

and the maximum efficiency is a thermodynamically-limited 83%.

(If the assumption that water stays in the liquid form is incorrect, the waste heat that must be rejected decreases because the vaporization of the water cools the stack).

### 3.1.2 Types of fuel cells

The classification of fuel cells is generally by type of electrolyte used. The electrolyte can be a

solid polymer, liquid acid or base, ceramic, or molten ionic salt. For reasons that will be detailed below, proton exchange membrane fuel cells (PEMFCs) are the type most suited for scooter applications.

#### *3.1.2.1 Phosphoric Acid Fuel Cell: well-developed, low density*

The fuel cell technology that has been in commercial (non-military) use for the longest time uses phosphoric acid, often in silicon carbide ceramic matrices, as the electrolyte. The phosphoric acid fuel cell runs at over 150°C, which increases catalyst activity. The higher temperatures are also necessary because phosphate anions adsorb on to the oxygen (reduction) electrode below 100°C, reducing catalytic performance.<sup>6</sup>

Phosphoric acid fuel cells accept either direct hydrogen or “reformat”, a mixture of hydrogen, carbon dioxide, water, carbon monoxide and possibly nitrogen and trace gases produced from the conversion of fossil fuels into hydrogen and carbon monoxide. Carbon monoxide mixed with the fuel (anode) flow is dangerous, because it can “poison” the catalyst. Basically, this means that active sites on the metal structure become filled with carbon monoxide molecules, making them unavailable for hydrogen catalysis; this is a problem with hydrogen fuel reformed from hydrocarbons, where the hydrogen is mixed with carbon monoxide. Carbon monoxide pollution in the air reaching the cathode is less of a problem, because here the concentration of oxygen and the oxidation potential are high; the oxidation of carbon monoxide to carbon dioxide proceeds rapidly and the catalyst is not poisoned although there is a slight drop in voltage. Depending on temperature, phosphoric acid fuel cells (PAFCs) are able to tolerate concentrations of CO in the fuel stream of up to 1-3%.<sup>7</sup> The output of a steam reformer is roughly double this value which is why an additional carbon dioxide cleanup step is needed.

For 5 kW applications, passive cooling (heat sinks and fins) may be sufficient to cool the system. The high temperatures also have the advantage of transporting the product water as steam instead of as liquid. The temperatures are low enough that noble metal alloy catalysts are required, on the order of  $0.2 \text{ mg}\cdot\text{cm}^{-2}$  on the hydrogen electrode and  $0.4 \text{ mg}\cdot\text{cm}^{-2}$  on the oxygen electrode.<sup>8</sup>

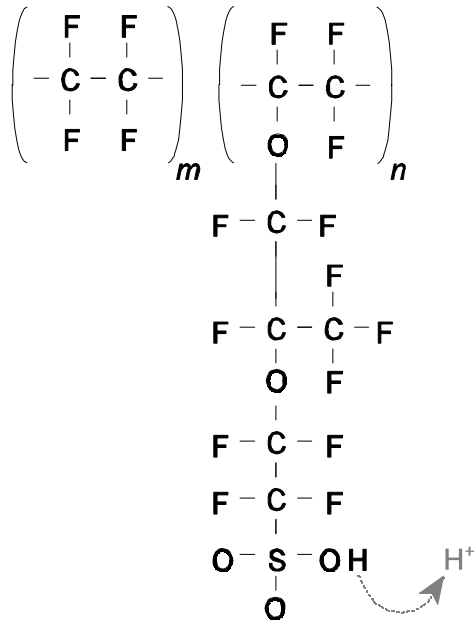
PAFCs have about a third of the performance of modern polymer electrolyte membrane fuel cells (PEMFCs), in terms of power per membrane area in  $\text{W}\cdot\text{cm}^{-2}$ , because PEMFCs have stronger acids in their electrolytes and because the thinner polymer membranes have much lower ohmic losses. Power densities are lower in PAFCs for another reason: the silicon carbide matrix that holds the phosphoric acid electrolyte must be a minimum of 0.1-0.2 mm thick for mechanical stability, increasing total stack size. Finally, PAFCs must be kept above  $45^\circ\text{C}$  even when not in use because below this temperature the acid solidifies and expands, risking damage to electrodes or silicon carbide matrix.<sup>9</sup> These two reasons of low power density and finicky temperature conditions explain why, after a few bus demonstrations, PAFCs have been relegated to stationary applications.

### *3.1.2.2 Proton Exchange Membrane Fuel Cell: for mobile applications, the best*

The type of fuel cell currently receiving the most attention is the PEM fuel cell; PEM stands variously for “proton exchange membrane” or “polymer electrolyte membrane”. The membrane is usually a perfluorosulfonic acid polymer. This is a polytetrafluoroethylene (PTFE, trade name Teflon) chain with side chains terminating in an  $\text{SO}_3\text{H}$  group. It is the hydrogen on this sulfonate group that dissociates from the polymer when wet and appears as protons in the solution; polymer acids have the advantage that the anion ( $-\text{SO}_3^-$  tail) is fixed in the electrolyte rather than dissolved..

One common PEM is Nafion, a polymer developed by DuPont in the 1960's for use as a separator in the chlor-alkali industry and now used for other industrial electrochemical purposes. It is sometimes classified with the compounds known as “superacids” because they are stronger than pure sulfuric acid. Nafion and similar “ionomers” are currently produced at the rate of 100,000 m<sup>2</sup> a year, and sell for about 600 \$/m<sup>2</sup>.<sup>10,11</sup> This is predicted to decrease to 50 \$/m<sup>2</sup> if production expands to 1 million m<sup>2</sup> per year (150,000 PEMFC automobile engines each year)<sup>12</sup>

**Figure 3.4 Nafion chemical structure**



The ratio of  $n$  to  $m$  (i.e. active sites to inactive chain monomers) determines the acidity of the electrolyte.

Polymer electrolyte membranes can be made extremely thin, less than 50 μm, making for densely packed stacks and, consequently, high power densities. The thinness of the polymer electrolyte also means high conductance and low ohmic resistance losses, for about three times the performance (in



$\text{W}\cdot\text{cm}^{-2}$ ) of PAFCs. The moderate conditions that the fuel cell runs under are also a benefit when compared to the alternatives - highly corrosive acids, or high temperature ceramics and molten salts.

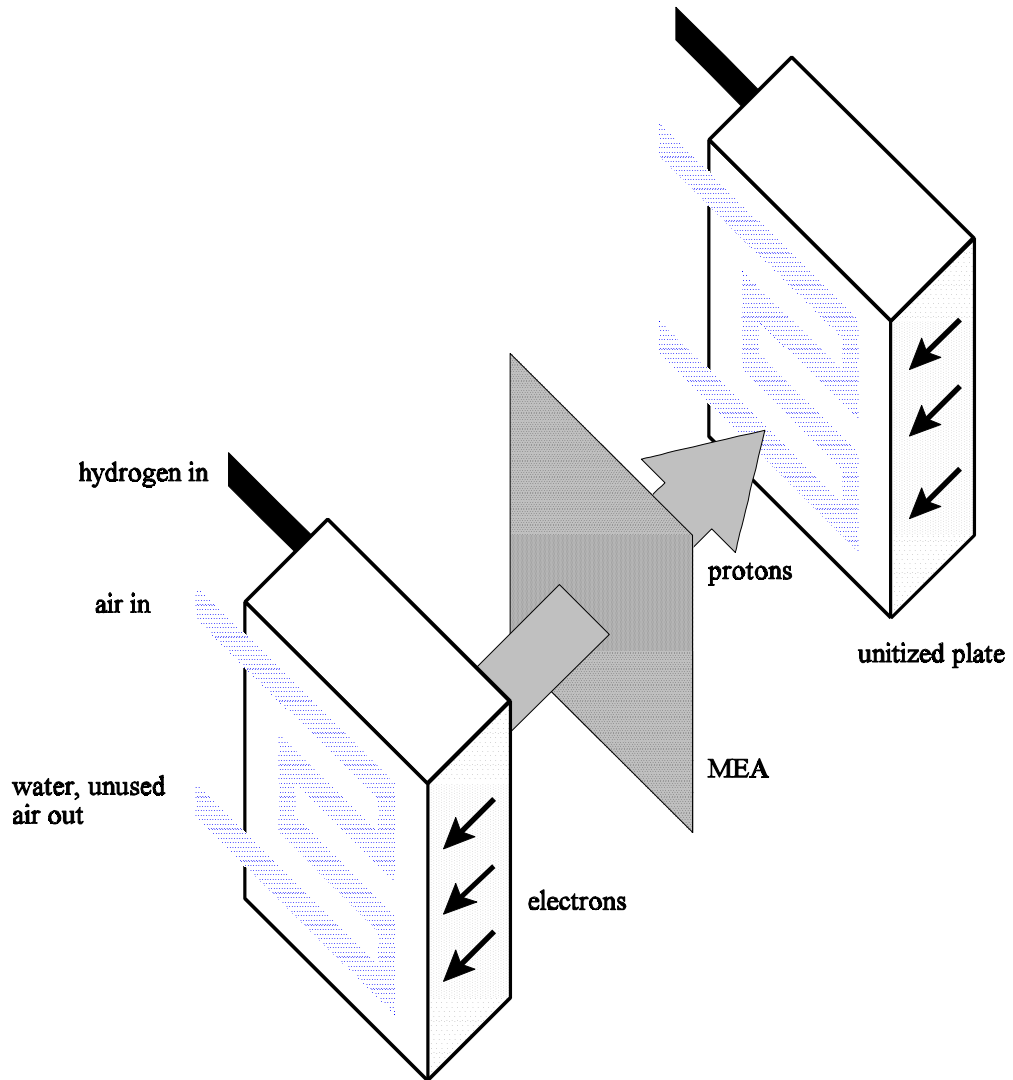
On the other hand, PEMFCs are especially vulnerable to “flooding”: the membrane becomes over-wet due to production of water at the cathode and diffusion of reactants is blocked. Also, platinum is required, less than  $0.4 \text{ mg}\cdot\text{cm}^{-2}$  for each of anode and cathode, mainly to resist the effects of carbon monoxide poisoning from impure hydrogen. Part of the reason is that PEMFCs operate at a relatively low temperature, under  $100^\circ\text{C}$ , because higher temperatures remove water from the membrane and damage it. At these low temperature catalysts are simply not as active. More catalyst is required at the cathode than at the anode due to the much lower activity of oxygen ionization.

Pt/Ru alloys are often used at the anode alloy in order to prevent carbon monoxide poisoning, because the presence of Ru changes the lattice constant of the resulting catalyst and makes carbon monoxide adsorption more difficult. PEMFCs significantly degrade in performance when operating on reformat of more than 50 ppm.

With maximum power densities of about  $600 \text{ mW}\cdot\text{cm}^{-2}$  and platinum costing about \$450 per ounce, this is a catalyst cost of 10.6 \$/kW.

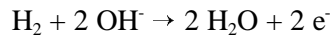
In the stack, the fuel cells are arranged so that ions (protons) pass through the membrane, while electrons are conducted through the separating graphite plates in the opposite direction.

Figure 3.5 Stack diagram

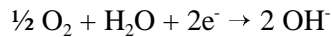


### 3.1.2.3 Alkaline Fuel Cells: poisoned by carbon dioxide

Alkaline fuel cells, which work at a temperature of about 100°C, are among the most efficient, and allow the use of less expensive catalyst materials like nickel because the use of an alkaline electrolyte and consequent high pH shifts the electrochemical potential to reduce activation overpotential. They have fairly high power densities. The anode reaction is:



The cathode reaction is:



The net reaction is the same as the PEMFC: the combination of hydrogen and oxygen molecules to form water. However, the ionic conductor here is the hydroxide anion rather than  $\text{H}^+$ . The electrolyte (typically potassium hydroxide, KOH) is either fixed in an asbestos matrix or pumped and circulated as a liquid. Power density is not as high as in a PEM fuel cell.

Another serious deficiency is that alkaline fuel cells cannot withstand carbon *dioxide*; carbon dioxide in the air or fuel streams reacts with the electrolyte to form potassium carbonates which can precipitate out. The content of  $\text{CO}_2$  in air was 353 ppm in 1990<sup>13</sup>, but modern AFCs can only tolerate 50 ppm<sup>14</sup>. This is fine for space applications where oxygen can be supplied in its pure form, but in ground vehicles powered by AFCs, scrubbers are needed to reduce the carbon dioxide level to acceptable levels. This is not practical for scooters, although Zevco, a British company, is working on a taxi fleet running on alkaline fuel cells equipped with chemical carbon dioxide scrubbers.<sup>15</sup>

#### *3.1.2.4 Solid Oxide and Molten Carbonate Fuel Cells: higher temperature*

For applications above 600°C, more exotic materials can and must be used for the electrolyte.

With a solid oxide fuel cell (SOFC), the electrolyte is a ceramic oxide and conduction takes place by oxygen ion ( $O^{2-}$ ) hopping through the electrolyte. Molten carbonate fuel cells use molten ionic salts (e.g.  $Li_2CO_3$ ,  $K_2CO_3$ , and mixtures thereof).

Both of these fuel cells find their utility in stationary power applications, where efficiency gains can be realized by using the exhaust stream and its high grade waste heat to drive a gas turbine bottoming cycle or provide cogenerated heat. These additional outflows would be wasted in a scooter which lack the room for additional “bottoming” cycles.

The high temperatures of these fuel cells offer the possibility of “internal reforming,” where natural gas and steam are introduced directly into the fuel cell and steam-reforming and water-gas cleanup occur automatically. SOFCs can even use carbon monoxide as fuel without reforming. The high temperatures mean that noble metal catalysts are not needed, but also bring with them their own materials problems.

Neither of these fuel cells has the high power density needed for vehicle power.

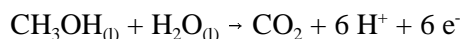
#### *3.1.2.5 Direct Methanol Fuel Cells: long-term promise*

A direct methanol fuel cell is an exception to the rule that fuel cells are categorized by their electrolytes; in this case, it is the fuel that defines the fuel cell. (Typically, the electrolyte used in conjunction with DMFCs is a PEM). Dilute methanol is flowed through the anode as the fuel and

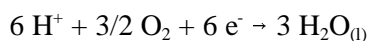
broken down to protons and electrons and water. Methanol is chosen because it is one of the few widely-available fuels that is electroactive enough to use in a fuel cell; ethanol can also be used but with poorer efficacy, due to its poorer electrical activity.

Much research is being done on direct methanol fuel cells, because a fuel cell run directly on liquid fuel would offer dramatic advantages in overall system density since neither low-density hydrogen nor bulky reformers would be needed. Methanol can be made relatively easily from gasoline or biomass, and although it only has a fifth the energy density of hydrogen by weight, as a liquid it offers more than four times the energy per volume when compared to hydrogen at 250 atmospheres.

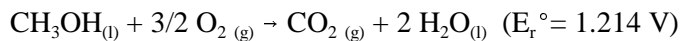
For a DMFC, the overall anode reaction is:



At the cathode,



The net reaction is the oxidation of methanol:



For the lower heating value reaction,  $E_r$  is 1.170 V, slightly less than hydrogen at 1.185 V. For each mole of methanol, six electrons are transferred, and this would seem far superior to the two electrons of a hydrogen PEMFC, but the comparison is properly with not one mole of hydrogen,

but one mole of methanol reformed into hydrogen. In the theoretical maximum case, three moles of hydrogen molecules can be reformed, so the total number of electrons are equal in each case.

Note that the presence of carbon dioxide means that an acid electrolyte must be used. Since the ion being exchanged is a proton, the DMFC can operate with a polymer electrolyte membrane.

One major problem is that the oxidation of methanol produces intermediate hydrocarbon species which poison the electrode. The other major problem is that the exchange current for methanol is much lower than that for hydrogen - by as much as six orders of magnitude.<sup>16</sup> This means that the oxidation of methanol at the anode becomes as slow as the oxygen electrode reaction, and large overpotentials are required for high power output. Also, there is high crossover of the methanol through the electrolyte, meaning that the fuel molecules diffuse directly through the electrolyte to the oxygen electrode. As much as 30% of the methanol can be lost this way, severely compromising power.<sup>16</sup>

As a result, maximum demonstrated power densities in 1998 were on the order of  $200 \text{ mW}\cdot\text{cm}^{-2}$  with air at 2.5 atm in a 2" x 2" cell, insufficient for current applications except very small portable fuel cells.<sup>17</sup> Platinum loadings were  $4 \text{ mg}\cdot\text{cm}^{-2}$ , almost a factor of ten greater than hydrogen-air fuel cells. Future improvements in catalyst and membrane design are expected to change this situation, with year 2000 goals of  $300 \text{ mW}\cdot\text{cm}^{-2}$  at  $1 \text{ mg}\cdot\text{cm}^{-2}$ .<sup>18</sup>

### **3.1.3 Stack characteristics**

The PEM fuel cell is the best for this, and many other, vehicle applications. The next step is to characterize how large a fuel cell would be needed to supply the demanded power. This is done

first by a comparison with published overviews of automobile fuel cell power, and second with a more detailed, ground-up model based on a Directed Technologies, Inc. (DTI) study.

#### *3.1.3.1 Fuel cell stack specifications*

The fuel cell stack is sized here by determining a standard motor voltage and connecting many fuel cells in series to create the desired voltage. Maximum current *density* is fixed by the properties of the membrane, but the total current can be increased by choosing cells with larger surface area. For a given nominal power output, a fuel cell that is oversized for that nominal power means that the power system is more often operating at a smaller fraction of maximum power - and thus at higher voltages and higher efficiency. On the other hand, it is expensive and often inefficient from an overall systems perspective to build such a heavy and expensive stack, especially since in road vehicles the maximum power is so infrequently required.

The process described above is carried out in section 4.4.1, after detailed power and performance requirements are derived in sections 4.1, 4.2, and 4.3. However, to give away the ending, the maximum gross power output is 5.9 kW for standard urban driving (5.6 kW net of parasitic power).

#### *3.1.3.2 Published results for automobile fuel cell stacks*

First, PEM fuel cell stack characteristics are estimated based on previous top-down studies for automobiles.

The PNGV (Partnership for a New Generation of Vehicles government/industry collaboration)

goals for fuel cell stack mass and weight are 0.35 kW/kg and 0.35 kW/L, by approximately the year 2000.<sup>19</sup> This is exclusive of auxiliary systems like radiators and blowers. The same source sets goals of 0.5 kW/L and 0.5 kW/kg by 2004. (For the 5.9 kW system studied here, that translates into 12 kg and 12 L). However, it should be noted that Ballard achieved 1 kW/L as early as 1996.<sup>20</sup>

The PNGV also defined year 2004 goals of 50 \$/kW net power for the fuel cell system (stack and auxiliaries) and an intermediate price target of 150 \$/kW by 2000.<sup>21</sup> Thus, for a 5.6 kW system, in five years the cost could be as low as \$280 if automotive-sized system costs scale down to the scooter size. This depends on significant cost reductions from current prices, which are on the order of \$1000/kW.

Ogden *et al* surveyed price estimates in the literature and found a price range of \$33 to \$100 per net kW for the fuel cell stack, and \$10 to \$20 per kW for the peaking power battery. The range cost estimates is thus \$185-\$560 for the 5.6 kW fuel cell-only scooter.<sup>22</sup>

### *3.1.3.3 Detailed construction*

The fuel cell engine itself is made of several cells electrically and physically connected in a box-shaped “stack”. Oxygen and hydrogen must be brought to the membranes where they can react, while the membranes themselves must be kept wet so that they can conduct the hydrogen ions (protons). Surplus water must be pushed out of the stack, and waste heat must be rejected from the stack to avoid overheating and membrane damage. The cells, which are made of electrically conductive graphite or metal, are constructed in series so voltages from each cell add up; the same current flows through the entire stack. The hydrogen and oxygen flow in molded manifolds



typically built off the side of the stack, and are divided into parallel feeds into the individual cells; water and exhaust gas are collected in another manifold and rejected to the atmosphere (the water may be recycled to humidify the incoming gases).

Essentially, each fuel cell in the stack contains an MEA, or membrane electrode assembly, which consists of the polymer ion-conduction membrane with flat electrode sheets attached to either side. Oxygen and hydrogen are channeled to the cathode and anode sides respectively in flow fields carved or pressed into plates that are next to the electrodes. These can be two separate plates, each serving a single electrode (“unipolar” design), or a single plate carved on both sides with flowfields can be used for two adjacent electrodes (“bipolar design”). The membrane must pass hydrogen ions but not electricity; the plates must conduct electricity, but not allow water, hydrogen, or oxygen to permeate through.

The DTI study examined a number of options with membranes of active area 116 cm<sup>2</sup> to 697 cm<sup>2</sup>, and calculated costs and weights for each of the sub components using design for manufacture and assembly (“DFMA”) techniques. Four possible cell designs were studied in the DTI report: unitized stainless steel; three-piece stainless steel; amorphous carbon; and carbon-polymer composite. The three-piece stainless steel cells were chosen here to estimate long-term, mass-produced cost estimates for the fuel cell stacks.

A detailed description of the stack size, weight, and cost analysis is provided in Appendix B. Essentially, the model was built from the bottom up, rather than simply extrapolating from the automotive-sized vehicles, although some of the figures are still based on the automotive model.

The MEA from DTI's model is 70  $\mu\text{m}$  thick in total. It consists of a 5  $\mu\text{m}$  composite membrane, sandwiched between 28  $\mu\text{m}$  thick layers of electrode (these electrodes consist of platinum deposited on carbon black which sits on an inert ionomer carrier, and then 25  $\mu\text{m}$  of electrically conductive porous backing, made of carbon paper impregnated with fluoropolymer like Teflon to repel accumulated water).<sup>23</sup>

Right now, typical membrane thicknesses are on the order of 50  $\mu\text{m}$  - 127  $\mu\text{m}$  for Nafion, and as low as 25  $\mu\text{m}$  for a newer Gore membrane. A prediction of 5  $\mu\text{m}$  is aggressive although it should be noted that, in DTI's model, the thinness of the membrane mainly reduces costs, not stack size.

Today's separator plates are made from graphite, which has low electrical conductivity but resists the corrosion caused by the electrochemical potentials in the cell. However, it is extremely expensive to machine flow field patterns into the graphite surfaces, and graphite itself is not inexpensive. (Machined graphite separator plates currently cost "as much as 200  $\$/\text{kW}$ "<sup>24</sup> ). Future prices are predicted to be as low as 5  $\$/\text{kW}$ , and cheaper material options include conductive polymers, impregnated amorphous carbon, and metal treated with anticorrosive coatings.

The three-piece cell design is chosen: in each active cell, one metal separator plate is matched with two separate, unipolar plates etched with flow fields.

51  $\mu\text{m}$  separator plate

76  $\mu\text{m}$  anode flow field

1000  $\mu\text{m}$  anode gasket

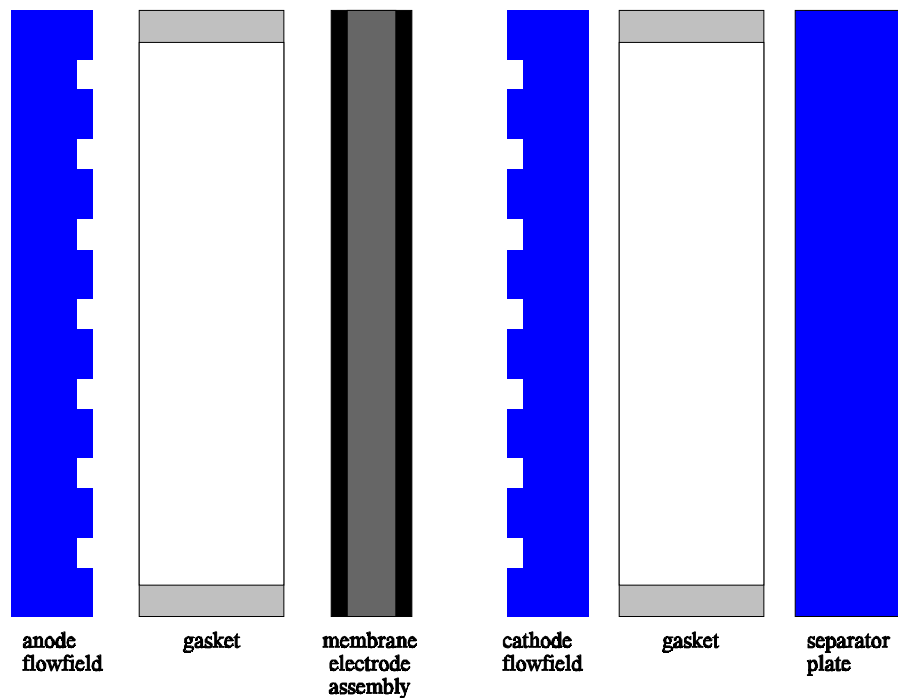
70  $\mu\text{m}$  MEA

76  $\mu\text{m}$  cathode flow field

1000  $\mu\text{m}$  cathode gasket

[repeat with next separator plate; total thickness 2.3 mm]

*Figure 3.6 Active Cell*



Each system requires cooling plates periodically interspersed between the active cells described above. The cooler cells allow flow of coolant within the stack, and are essentially flow fields through which only water flows. The cells are made of the same electrically-conductive stainless steel to allow bulk conduction of current. The reason for using cooler cells of the same design as the ordinary (“active”) cells is to increase the number of identical components and, again, decrease manufacturing costs. A cooler cell to active cell ratio of 1:2 is defined here.

A three-piece metallic cooler cell consists of:

51  $\mu\text{m}$  separator plate

76  $\mu\text{m}$  coolant flow field

1000  $\mu\text{m}$  gasket

[repeat with next separator plate; total thickness 1.1 mm]

In addition to the repeating cells, the stack requires an electrically insulating plastic housing; tie rods to hold the cells together; current collectors at the ends of the stack to conduct electricity to the power system; and insulators and endplates over the current collectors.

#### 3.1.3.4 Detailed construction results

The results are summarized below for three different fuel cell stack sizes, each 56 cells long for a total voltage close to 48 V.

*Table 3.1 Stack size, weight, cost summary*

	<b>5.9 kW</b>	<b>3.3 kW</b>	<b>1.1 kW</b>
<b>membrane active area</b>	170 cm <sup>2</sup>	100 cm <sup>2</sup>	35 cm <sup>2</sup>
<b>total mass of non-repeat units</b>	5.1 kg	3.6 kg	3.3 kg
<b>total mass of repeat units</b>	2.8 kg	1.8 kg	0.8 kg
<b>total stack mass</b>	7.6 kg	5.4 kg	4.0 kg
<b>total stack volume</b>	7.8 L	5.3 L	3.2 L
<b>stack power density by weight</b>	0.78 kW/kg	0.62 kW/kg	0.27 kW/kg
<b>stack power density by volume</b>	0.76 kW/L	0.62 kW/L	0.34 kW/L
<b>total stack cost</b>	\$244	\$161	\$124
<b>cost of power</b>	42 \$/kW	47 \$/kW	103 \$/kW

These are long-term mass-produced prices. In comparison, a Ballard 37 kW stack available today has power densities of 1.1 kW/L and 0.8 kW/kg, so the results above are not overly ambitious.<sup>25</sup>

For comparison purposes: a simplistic curve-fitting to the DTI model's results for automotive fuel cell engines gives lower costs of \$176, \$125, and \$96 - about 20% to 30% lower. See Appendix B for more details.

### **3.1.4 Gas flow management**

In addition to the stack itself, several subsystems are needed in a fuel cell power plant. One of the most important ones is the gas flow subsystem. Oxygen and hydrogen are introduced into the fuel cell system at the appropriate flow rate required for the current at any given moment; this requires a variable-flow system if the stoichiometry is to be kept constant. Even in an “atmospheric-pressure” system, some pressure over atmospheric is needed in order to push the gases through the often-serpentine passages carved into the flow plates, and to force liquid water out of the same passages. This additional pressure is on the order of 0.1 to 2.0 psi (0.7 to 13.8 kPa) above atmospheric; IFC (International Fuel Cells) quotes 0.8 psi.<sup>26,27</sup>

A minimum flow speed of 0.35 m/s is needed to eliminate product water, and a Schatz Energy Research Center patent estimates flow velocities at up to 7 m/s.<sup>28, 31,28</sup> Due to the fact that the cathode reaction is much slower than the anode reaction, oxygen is often supplied at a higher-than-stoichiometric flow rate. The ratio of air flow rate to the minimum flow rate required for stoichiometric oxygen-hydrogen reaction is often 2.0 or higher in order that the concentration of oxygen in the air not drop too much as it passes through the flow field, and the excess air also helps to push product water generated at the cathode out of the fuel cell.

An air filter is needed to prevent foreign objects from being taken into the fuel cell.

Hydrogen is supplied dead-ended in the design proposed here. This means that there is no outlet to the anode side; the pressure is simply allowed to equilibrate in the stack to match the pressure regulator output. Electrochemical consumption is matched by replacement from the hydrogen store. The result is 100% hydrogen utilization. This technique can only be used for pure hydrogen vehicles because the anode stream from reformed hydrocarbons or ammonia would contain inerts ( $N_2$ ,  $CO_2$ ,  $H_2O$ ) and poisons ( $CO$ ) that would build up at the anode dead end. Dead-ended fuel cells still need to vent occasionally in order to purge impurities that may have entered the fuel cell; this involves opening the anode exhaust valves for a brief period and allowing the hydrogen to flow directly into the atmosphere for a very brief time. Effective utilization is slightly less than 100% for this reason, although in this study this loss is assumed to be negligible. (Stacks running open-ended have hydrogen utilizations of approximately 85% unless pure hydrogen is recycled.)

To manage the air flow, blowers are briefly discussed below. Then, the utility of pressurized operation is analyzed.

#### *3.1.4.1 Blowers*

Blowers are used in atmospheric systems to draw air into the fuel cell; no corresponding device is needed for the hydrogen side, because in all current designs the hydrogen is kept under pressure higher than the operating pressure of the fuel cell, and expands as it is released from the storage container or produced above atmospheric pressure in a reformer. The blower is typically powered electrically from the fuel cell output, with a battery required for startup.

The blower power required is:

$$\dot{W} = \frac{\Delta P \dot{V}}{\eta}$$

where  $\eta$  is the blower efficiency. For the power requirements of a 5 kW fuel cell (2.0 psi pressure drop and a flow rate of 15.6 cubic feet per minute) and a 50% blower efficiency the power consumption is 200 W.

An industrial heavy-duty blower that could be used to provide the required output is the Ametek 5.7" BLDC three-stage blower, model 116638-08, with a catalog sale price of \$430.<sup>29</sup>

#### *3.1.4.2 Compressors*

Compressing the air input increases the concentration of oxygen per volume per time – its effective partial pressure – and thus increases the fuel cell efficiency. This means that a smaller and lighter fuel cell stack can be used, at the price of parasitic power required by the compressor and increased cost. In addition, the drop-off in voltage caused by mass transport problems is delayed until higher current densities. Another benefit of higher pressures is that, for the same molar flow rate, a lower volumetric flow rate can be used. Thus, humidification is easier because less water is needed for saturation (per mole of air). Finally, flow-field design is less restrictive because larger pressure drops can be tolerated in the flowfield.

Since most of the hydrogen storage techniques involve pressurized hydrogen, it is not be difficult to obtain a matching pressurized hydrogen stream; in any case, a typical PEM can tolerate a pressure difference of about 0.5 bar for Nafion-115.<sup>30</sup>

In a tightly-integrated system, the compressor can be powered mechanically as a turbocharger, using a shaft attached to a turbine running off the exhaust from the fuel cell. This allows recovery of some of the expansion work. On the other hand, the system may be simpler if the compressor is powered only by an electric motor, with separate battery for startup purposes.

Compressors on the order of 0.5-10 kW are difficult to find and generally inefficient.<sup>31</sup> The Department of Energy has a goal of 3 kg, 4 L, 68% efficiency, and \$200 at 70-80 grams/second for a turbocompressor/expander for a 50 kW fuel cell system.<sup>32,33</sup> Note that this is ten times the flow rate required for a 5-6 kW scooter, and efficiency decreases dramatically with “turn-down” (operating below the design point), so actual efficiency will likely be lower. Also, for the low flow rates involved, variable speed positive-displacement compressors (rather than turbomachines) are typically used and efficiency may be lower for that reason as well. The DOE target size and weight are quite low for the benefit in voltage, but cost would be significant when compared to the cost of the total system.

The net benefit of compression for the scooter system is analyzed in section 4.6 in the system modeling chapter.

### **3.1.5 Water management**

Water is vital to fuel cells in that the electrodes and the electrolyte must be kept wet in order to allow proton conduction through the acid medium. Water enters the system from externally humidified hydrogen and/or air streams and generation at the cathode by the electrochemical reaction. Due to hydrogen bonding, on average 1 to 2.5 water molecules are dragged along with each proton as it migrates from the anode to the cathode; this is known as “electro-osmotic drag.”



Water also flows in the other direction due to back-diffusion, since the concentration of water in the cathode electrode is much higher than at the anode electrode. Water exits the system with the cathode exhaust as blown-out liquid or vapour.

The greatest danger posed by water is that of drying out. Loss of water can dry out the electrodes or the membrane, leading to a runaway in overheating and current loss and damage to the membrane. On the other hand, if too much liquid water accumulates at an electrode, it can block the diffusion of gas into that electrode, preventing dissociation and slowing down the overall conversion to electricity. Drops in current density are often the symptoms of flooding.

Voltage (efficiency) is higher with humidified flow than with unhumidified reactant streams. In test stations, “external” humidification is typically achieved by bubbling the reactants through a reservoir of water. IFC has demonstrated “internal humidification” by absorbing water into porous bipolar separator plates, and using this reservoir of water to replenish the water in the electrodes and electrolyte.

Various methods have been proposed to remove water from the cathode. If the temperature and flow rate are high enough, the warmed oxidant can vaporize the product water and carry it away as water vapor. If the oxidant pressure and flow rate are high enough, the liquid water is physically pushed out, although flow rates that are too high will dry out the membrane and anode. Finally, a separate path of hydrophilic polymer can be used to “wick” (draw by capillary action) the water from the cathode back to the anode side, which tends to dry out faster.

Fuel cells running with a dead-ended fuel supply cannot humidify the anode flow, because water would accumulate in the hydrogen dead end. So, to prevent the anode from drying out, the

incoming *air* flow is humidified by passing it over a wetted polymer wicking water from a reservoir, or through a water bottle. Back-diffusion is allowed to carry the moisture through the membrane back to the anode, and the thinner the membrane, the more quickly back-diffusion can operate. If temperatures are low, this diffusion can be enough to remove the need for external humidification.

Water in the fuel cell has to be deionized; this can be done by forcing the water through a filter or by supplying the vehicle with deionized water only. In the case where all water needs are supplied by condensation and then recirculation of the product water, deionization is not a concern. In the scooter system, without room for a condenser and second cooling fan, the water may just be exhausted.

### **3.1.6 Heat**

The designed operating temperature of the fuel cell affects various factors. A higher operating temperature means that more of the product water is vaporized, so that more waste heat goes into the latent heat of vaporization and less liquid water is left to be pushed out of the fuel cell. Higher temperatures also mean faster kinetics and a voltage gain that in general exceeds the voltage loss from the negative *thermodynamic* relationship between open-circuit voltage and temperature. Heat rejection is also abetted at higher temperatures due to the larger difference between the fuel cell temperature and ambient temperature. On the other hand, lower stack temperatures mean shorter warmup times for the system as a whole, and lower thermomechanical stresses. Corrosion and other time- and temperature-dependent processes are retarded, and much less water is required for saturation of input gases.

The upper limit of operation for PEMFCs is about 90°C because water evaporates from the membrane and performance drops quickly; permanent damage can occur to the membrane. At Princeton and various other places, membranes are being developed that can handle higher temperatures while retaining the high power density of PEMFCs. This is being attempted by making novel electrolyte that are composites of Nafion with materials that hold water more tightly and prevent evaporation: proton-conducting glasses and hydrated oxides of silicon. Another technique is to replace water in Nafion with different chemicals that have higher boiling points.<sup>34</sup> The primary objective is higher CO tolerance (since the catalysts are more effective at higher temperatures) without drastic loss of performance.

Another heat-related issue is preheating of the inlet air and hydrogen. This is advantageous to prevent flooding at the inlet at the part of the stack closest to the air entry. This is the point at which the air is coolest, having not yet warmed up to the full stack temperature, and has the highest concentration of oxygen since the air has not yet been depleted of oxidant. Cathode water production is highest here, and the cool air saturates with water easily if not preheated.<sup>35</sup>

Preventing overheating is described in greater detail. Under the most strenuous conditions, a 5.9 kW fuel cell operating at 50% efficiency produces 5.9 kW of waste heat - a significant instantaneous load to manage. However, as will be shown later, the *average* fuel cell load for a scooter in a city driving cycle is one-tenth of the maximum, and at this power level efficiencies are higher than at maximum load. The thermal mass in the system damps out the peaks when the transient heat generations are converted to temperature rises, as analysis in section 4.4.4.3 shows.

Cooling can be achieved through a number of means. First, the evaporation of some of the product water at the cathode absorbs some heat. Second, active cooling with air or liquid coolants can be

used to transfer heat to radiators. Third, passive cooling of the fuel cell can be performed with cooling fins and heat sinks. Finally, the fuel cell might be coupled with subsystems that absorb heat like turbine reheaters and metal hydride containers.

#### *3.1.6.1 Active cooling*

Pumping a coolant fluid (either air or water) through cooling passages within the fuel cell stack would allow much heat to be removed. This heat would have to be dissipated at a radiator, so in addition to the pumping energy, a fan would be needed to increase convection over the radiator.

Requirements include noncorrosive coolant fluid; a pump to circulate the fluid; seals; a radiator and radiator cooling fan; a deionizing filter; and a surge tank. Researchers at the Institute of Integrated Energy Systems at the University of Victoria estimated the power required by the fan blowing over the radiator at 83 W for a 5 kW Ballard Mark V stack.<sup>36</sup>

Radiator and fan size, weight, and cost are described in more detail in section 4.4.4.4, after the radiator cooling capability requirements are calculated.

#### *3.1.6.2 Passive cooling*

Cooling using fins *without* a powered fan blowing over them is virtually impossible to achieve at sizes greater than 50 W because of the limited surface area and the low temperature difference between the maximum  $\sim 80^{\circ}\text{C}$  temperature of PEMFCs and the ambient temperature, which in Taiwan can be as high as  $40^{\circ}\text{C}$ . However, forced air ventilation over fins attached to the fuel cell stack is possible for cells of the proper narrow aspect ratio, as H Power fuel cell stacks have

demonstrated. Less total cooling air flow is required than for water cooling because the intermediate (water circulation) step is eliminated, and stack weight and volume are saved by not having to interpose cooler cells between active cells. On the other hand, some kind of heat conduction path is needed to get from the stack to the environment. Also, the heat capacity of air is far lower than water, and when coupled with the small change in temperature from fuel cell to ambient environment, the result is poor heat transfer.

### *3.1.6.3 Boiling refrigerant*

Using a closed-loop refrigerant that boils at the fuel cell operating temperature (50°C - 80°C) would allow a great deal of thermal energy to be withdrawn from the stack. In addition, the pressure of the vaporized coolant (in conjunction with a check valve) could be used to drive the coolant cycle without requiring a pump, minimizing parasitic losses. A fan would likely still be needed on the condensation (radiator) side, but otherwise the system would feature automatic control without electronics.

Active cooling with a liquid coolant loop is chosen here, to be certain of sufficient cooling. Air cooling is unlikely to be successful in a stack as large as 5.9 kW, as the available surface area is low. Heat issues are discussed in more detail in section 4.4.4.

## 3.2. Fuel for the fuel cell

---

The PEMFC must be supplied with hydrogen. This hydrogen can be stored as hydrogen, but it can also be “reformed” from other chemicals using an onboard chemical processor. The advantages of the latter are that liquid fuels, with their high energy density (as a function of volume) and easier distribution, can be used. However, reforming requires additional equipment which comes at a premium on a small vehicle. Also, reformers usually produce some pollution on their own but this is trivial compared to combustion engines.

Modeling results from sections 4.5.1 and 4.4.1.4 will show that the fuel requirement for the scooter to travel 200 km at 30 km/h is 250 grams of hydrogen, and a maximum flow rate of approximately 0.05 moles  $\text{H}_2 \cdot \text{s}^{-1}$  is needed at the upper limit of 5.9 kW of gross power.

### 3.2.1. Reformed fuels

The standard technology predicted for the first commercial fuel cell cars is hydrogen reformed onboard from liquid fossil fuels like methanol or gasoline, because these fuels are widely available and have excellent energy densities. Some interesting other technologies, like producing hydrogen from dissolving certain chemicals in water, and reforming ammonia into hydrogen, are mentioned here because they might find use in the smaller scooter application.

#### 3.2.1.1. Hydrocarbon reforming.

Liquid hydrocarbon fuels contain a great deal of energy per unit volume, far more than hydrogen,

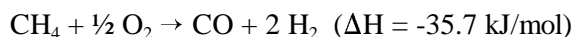
and are cheaply available. The two major candidates for fuel cell vehicles are methanol and gasoline. Methanol produces less carbon dioxide and reduces long-term oil dependence, and is easier to reform; gasoline has extensive existing production and distribution infrastructure. Natural gas is another possibility.

**Table 3.2 Fuel gravimetric and volumetric energy densities, lower heating value basis**

	<b>by mass</b>	<b>by volume</b>
Hydrogen gas, atmospheric pressure	120 MJ/kg	11 kJ/L at STP
Compressed hydrogen gas, 3600 psi	120 MJ/kg	2,700 kJ/L at 3600 psi
Gasoline (approximate)	44 MJ/kg	31,800 kJ/L liquid
Methanol	20 MJ/kg	15,900 kJ/L liquid
Natural gas (pure methane)	50 MJ/kg	36 kJ/L at STP
Compressed methane, 3600 psi	50 MJ/kg	8,700 kJ/L at 3600 psi

Data from Electric Vehicle Technology, CARB report <sup>37,38</sup>

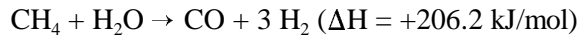
There are two major methods of reforming hydrocarbon fuels: partial oxidation (“POX”) and steam reforming. Partial oxidation is partial burning of the fuel to produce carbon monoxide and hydrogen. It is exothermic. To pick a sample fuel, if methane is partially oxidized:



Gasoline partial oxidation proceeds in essentially the same way. Partial oxidation requires high temperatures, 900°C - 1500°C, but can handle a wider variety of fuels than steam reforming.

Steam reforming combines the fuel with steam to produce the same products, and is endothermic.

The steam reforming equivalent of the reaction above would be



A steam reforming system is more efficient because waste heat from the later processes can be recycled as input into the endothermic steam reforming process (for example, if unused hydrogen in the anode exhaust is burnt). Steam reformers also produce more hydrogen because some comes from the water.

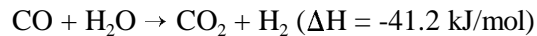
In general, partial oxidation is the simpler system because of the fewer heat integration and water management issues; it has lower capital costs for this reason. Partial oxidation reformers also have superior startup times, fuel flexibility, and may have faster response times. However, partial oxidizers for vehicles run on air so much inert nitrogen flows through; flow rates are higher and thus the downstream reactors like the water-gas shift and the PROX must be larger; also, the concentration of hydrogen in the reformat is lower in POX reactors than it is for steam reformers.

*Table 3.3 Steam reforming versus partial oxidation*

	<b>Partial Oxidation</b>	<b>Steam Reforming</b>
PROS	<ul style="list-style-type: none"> <li>• Simpler system</li> <li>• Fast response time</li> <li>• Greater fuel flexibility</li> </ul>	<ul style="list-style-type: none"> <li>• Theoretically more efficient</li> <li>• More hydrogen in reformat (higher fuel cell efficiencies)</li> </ul>
CONS	<ul style="list-style-type: none"> <li>• Air intake means greater flow rates, larger components</li> <li>• Less efficient</li> </ul>	<ul style="list-style-type: none"> <li>• Slow response time (several seconds)</li> <li>• Catalysts needed</li> <li>• Cannot handle gasoline</li> <li>• Capital-intensive heat exchangers necessary</li> <li>• H<sub>2</sub> burners, if needed, add complexity</li> </ul>



The next step in either process is the water-gas shift reaction. Here, most of the remaining carbon monoxide is reacted with water to produce additional hydrogen. A typical conversion is from 7.1% CO in a steam reformer's output (or 46.1% in from a partial oxidation reactor), to 0.5% coming out of the water-gas shift reactor.<sup>39</sup> Essentially,



There is one other important issue: the fuel cell must be optimized to accept an anode fuel stream that can be as low as 40% hydrogen for POX, or 75% hydrogen for steam reforming. The lower amount of hydrogen in either case means that fuel cell efficiency is lowered. Also, water must be either carried to supply the water-gas shift reaction (and any steam reformer), or recirculated from the exhaust. The total water needed is on the order of 3 grams per gram of H<sub>2</sub> for partial oxidation, and 4.5 grams per gram of H<sub>2</sub> for steam reforming.

CO poisoning is an important issue for polymer electrolyte membrane fuel cells, because the CO poisons the platinum (or other) catalyst on the electrode, reducing voltage at a given current density. Thus, for the same power output, a fuel cell running off reformed hydrogen must be sized larger. It is difficult to completely eliminate CO from the reformer exhaust, and fuel cells can only tolerate at most 50 ppm CO before efficiency drops dramatically, so a final "cleanup" step is required even after the water-gas shift. A preferential oxidizer ("PROX") or similar cleanup device is needed to perform CO removal. (A PROX is so named because it, due to the catalyst microdesign, it "prefers" to oxidize carbon monoxide rather than hydrogen; PROX efficiencies are often measured in terms of how much hydrogen is must be sacrificed to reduce CO down to acceptable levels.)

The amount of hydrogen that can be produced by reforming various hydrocarbons is listed below for both steam reforming and partial oxidation; as modeled, both processes include a water gas shift reaction to create more hydrogen from shifting carbon monoxide. The results are listed as effective hydrogen concentrations in the fuel; due to inefficiencies not all of the hydrogen can be recovered, but on the other hand, some of the weight fractions are greater than the fraction of hydrogen in the fuel molecules themselves because much hydrogen comes from the water.

**Table 3.4 Hydrogen output from reformed hydrocarbon fuels**

Fuel	Formula	Steam reforming			Partial oxidation		
		wt% H <sub>2</sub>	g H <sub>2</sub> per L <sub>fuel</sub>	mols H <sub>2</sub> O per mol fuel	wt% H <sub>2</sub>	g H <sub>2</sub> per L <sub>fuel</sub>	mols H <sub>2</sub> O per mol fuel
Methanol	CH <sub>3</sub> OH	19%	150	1.0	13%	100	0.0
Ethanol	C <sub>2</sub> H <sub>5</sub> OH	26%	209	3.0	22%	168	2.0
Methane (LNG)	CH <sub>4</sub>	50%	205	2.0	38%	151	1.0
Gasoline	C <sub>8</sub> H <sub>15.4</sub> (approx.)	43%	301	16.3	28%	200	8.1
Diesel fuel	C <sub>14</sub> H <sub>25.5</sub> (approx.)	42%	357	28.3	28%	231	14.2

Data from CARB study.<sup>40</sup>

Excellent overall weight fractions and hydrogen densities can be achieved in the fuel, but note that this does not include the additional weight of reformer equipment required, nor the extra water that is needed. Reformers for automobiles are predicted to cost 16-25 \$/kW for 50 kW sized stacks, but there is little data on pricing so far.<sup>41</sup>

The fuel cell industry is split on whether reformed methanol or gasoline will succeed first; methanol reforms with greater efficiency, but gasoline is perhaps easier to distribute (although it should be

noted that only gasoline free of detergents, sulfur, and other additives should be run through reformers. Sulfur would poison the reformer, PROX, or fuel cell catalysts and the effects of elements other than carbon, hydrogen, nitrogen, and oxygen passing through the reformer may be negative. Gasoline is likely to be reformulated for fuel cell cars running on reformed gasoline.)

The scooter design is extremely volume- and weight- sensitive, and bulky and complex heat exchangers are to be avoided, so if reformers make sense at all, a less efficient POX is superior.

### *3.2.1.2 Methanol reforming example*

Methanol reforming is discussed as an example of hydrocarbon reforming for the scooter. This most simple alcohol ( $\text{CH}_3\text{OH}$ ) is often cited as a leading candidate for fuel cell vehicles, because as a liquid it has high energy density, and because it is easier to reform than gasoline. It contains 12.5% hydrogen by weight.

The figures for a HotSpot POX reformer are given below. Johnson Matthey predicts an additional 20% volume for a PROX on top of that required by the POX, and 95% efficiency for this second stage, with overall efficiencies of 89%.<sup>42</sup> Fuel cells running on reformat cannot be operated dead-ended, so hydrogen utilization at the anode decreases to about 85%, for a total efficiency of 76%. The reduced hydrogen content in the reformat output (when compared to pure hydrogen) reduces the voltage of the fuel cell by approximately 0.128 volts per  $\text{A}\cdot\text{cm}^2$ , or roughly 20% at maximum power output.<sup>43</sup>

*Table 3.5 Reformer performance*

<b>reformer volume</b>	7.2 L
<b>reformer weight</b>	9.5 kg + cleanup unit weight
<b>hydrogen output after cleanup</b>	1.36 L/s
<b>hydrogen output</b>	0.061 mol•s <sup>-1</sup>
<b>fraction of hydrogen in output</b>	43%
<b>fraction of CO in output</b>	8 ± 5 ppm
<b>overall efficiency</b>	76%
<b>output per mole of methanol</b>	2.3 mol H <sub>2</sub>

At this production rate, 55 moles of methanol would be needed for the required 250 grams of hydrogen gas output. This corresponds to 1.8 kg of methanol, and a volume of 2.2 L, much less than a compressed gas cylinder or a metal hydride hydrogen adsorption device. The total volume is only 9.4 L, for POX and PROX and fuel tank; the total weight of the system is 11.3 kg plus the weight of the PROX. Assuming an 8 kg preferential oxidizer, and considering the reformer and PROX and fuel tank as a single “hydrogen storage system” produces densities of 1.3 wt% and 26 g/L, measured in terms of hydrogen output.

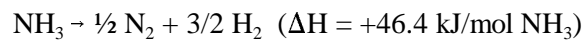
### *3.2.1.3. Ammonia*

Ammonia reforming is an interesting option that is somewhat different from the standard fossil-fuel reforming ideas, since it offers clean combustion from a chemical feedstock that is commercially available as a fertilizer. Fuel cell companies like Analytic Power and H-Power have developed prototypes running on liquefied ammonia.

Ammonia contains 17.6% hydrogen atoms by weight. This is as good as POX-reformed methanol

and with the advantage that the only products of ammonia reforming are hydrogen and nitrogen gas, ammonia would seem to be an excellent carrier for hydrogen. Also, ammonia is easily liquefied under pressure, and at a liquid density of 601 g/L at 300 K, equivalent to an H<sub>2</sub> volumetric density of 55 g / L. This liquefaction requires a pressure of only 10 bar at 300 K.

In principle, the ammonia cracking reaction is



The reaction takes place at over 400°C, which requires an external heat source since the exhaust from a typical proton exchange membrane exits at only 80°C. Traditionally, some of the hydrogen in the reformer's output stream is burned to provide the working temperature for the reformer and to provide the heat needed for cracking, although it is possible to tune the anode utilization of the fuel cell so that the exhaust stream from the fuel cell has enough heating value from the unconsumed hydrogen to supply the required heat if burned. The reformer efficiency, measured as the fraction of product hydrogen that does not need to be burned, is at most 70% and the system cannot be run dead-ended, so that there is a 15% anode utilization penalty.<sup>44</sup>

Fuel cell company Analytic Power has created an ammonia reforming system called the "A-Cracker". The system weighs 6 lbs, and has dimensions of 4" x 2.5" x 12", and operates at 60% efficiency (overall anode utilization efficiency of 51% due to incomplete consumption of hydrogen at the anode). The system consists of a dissociator, hydrogen burner, and regenerator for recycling heat. The maximum flow rate is 6 standard liters of ammonia per minute, which translates to 0.0040 net moles/s of hydrogen (enough hydrogen for a 500 W<sub>e</sub> alkaline fuel cell).<sup>45</sup>

For 5.9 kW, and assuming a lack of economies of scale, the reformer would require 33 kg of equipment with a volume of 22 L in addition to storage of the ammonia. The ammonia itself would take up about 2.2 kg and 3.7 L not including the tank itself. The system mass would be 35 kg and 26 L, for quite poor system hydrogen densities of 0.57 wt% and 7.7 g/L.

A major problem is the undissociated ammonia concentration in the product gas. Although the concentration is less than 50 ppm, this is still enough to damage fuel cells with acid electrolytes, so an acid scrubber is needed to remove the final traces of ammonia gas from the cracker. Also, ammonia is toxic; spills and evaporative emissions could be dangerous in a different way than gasoline or hydrogen spills, as inhaled ammonia damages the lungs.

Ammonia infrastructure exists for agricultural (fertilizer) use in many areas of the world.

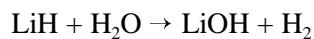
Ammonia sells for roughly \$1 per pound.<sup>46</sup> As a fuel, this makes it extremely expensive: at 120 MJ/kg of hydrogen lower heating value and 50% reforming efficiency, this is equivalent to a cost of 205 \$/GJ of hydrogen lower heating value, about ten times the cost predicted for hydrogen reformed from hydrocarbons in large centralized plants. This expense means that ammonia cannot be considered a viable option for scooters.

#### *3.2.1.4 Chemical hydride energy storage*

Hydrogen fuel can also be produced by chemical reaction with solid “chemical hydrides”. This technique lies somewhere between the metal hydrides and reforming, but is included here in the reforming section.

Chemicals like lithium hydride, lithium aluminum hydride, and sodium borohydride can be

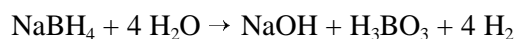
combined with water to evolve hydrogen gas (exothermically):



$$(\Delta H = -312 \text{ kJ}\cdot\text{mol}^{-1} \text{ LiH})$$



$$(\Delta H = -727 \text{ kJ}\cdot\text{mol}^{-1} \text{ LiAlH}_4)$$



These compounds are lighter than the reversible metal hydrides, and release more hydrogen because hydrogen is liberated from the water reactant. The three example chemical hydrides and their hydrogen storage capabilities are reproduced below.

**Table 3.6 Chemical hydride comparison**

	<b>LiH</b>	<b>LiAlH<sub>4</sub></b>	<b>NaBH<sub>4</sub></b>
<b>hydrogen-to-hydride ratio (wt%)</b>	25.2%	21.1%	21.3%
<b>hydrogen-to-hydride plus stoichiometric water ratio (wt%)</b>	7.7%	7.3%	7.3%
<b>hydrogen-to-system ratio (wt%), assuming 20% additional weight</b>	6.4%	6.1%	6.1%
<b>mass of hydride powder needed for 250 g hydrogen output</b>	980 g	1177 g	1173 g
<b>cost for mass of hydride given above (laboratory-scale pricing)</b>	\$268	\$503	\$178

Data is from Browning *et al.*,<sup>47</sup> with the exception of cost information which is from laboratory catalogs: Aldrich for the LiAlH<sub>4</sub> and Alfa Aesar for the others.<sup>48,49</sup>

The weight fraction is much higher, and the system requirements for containment are much less since the partial pressure of hydrogen over the hydride is low (1-10 atm). Browning *et al* estimate an extra 20% “for the weight of the hydrogen and water cylinders, mixing device and control valves.” For example, for the LiH to produce 250 grams of hydrogen, 0.98 kg of powdered hydride and a 2.2 kg tank of water would be needed. An additional 200 g of control and mixing systems would be needed.

Packaging the chemical hydrides in small subunits would make fuel distribution easy; if properly and safely contained, they could even be sold in convenience stores. Containment is not a trivial problem; the hydrides must be protected from water in liquid or vapour form that might cause an extremely exothermic reaction and ignite the released hydrogen. One other issue is that the scooter accumulates hydroxides which must be collected and safely disposed of, or better, reprocessed. Finally, the *less* exothermic of the two reactions, that for LiAlH<sub>4</sub>, produces 182 kJ of heat per mole of H<sub>2</sub> released. At maximum fuel cell power, when 0.05 moles of hydrogen are consumed every second, over 9 kilowatts of heat are generated! This is an enormous amount which exceeds that produced by the fuel cell itself, and makes for a large heat rejection problem.

As for cost, the prices are currently for small quantities of chemicals (2 kg maximum) produced at high (>95%) purity for experimental purposes. If chemical hydrides were actually to be used for vehicles, this price would have to decrease significantly. Also, the waste solution left after the reaction would be reprocessed and the cost would be expected to be lower than that for manufacturing a fresh batch of chemical hydride powder.

This type of technology is not well developed and tall barriers of cost and safety must be overcome if chemical hydrides are to be seriously considered for hydrogen vehicles. The exothermicity of the



reaction appears to be wasted in the scooter, where the primary purpose of heat management is to get *rid* of heat. They do offer the tempting possibilities of extremely high energy densities and easy distribution in convenient units.

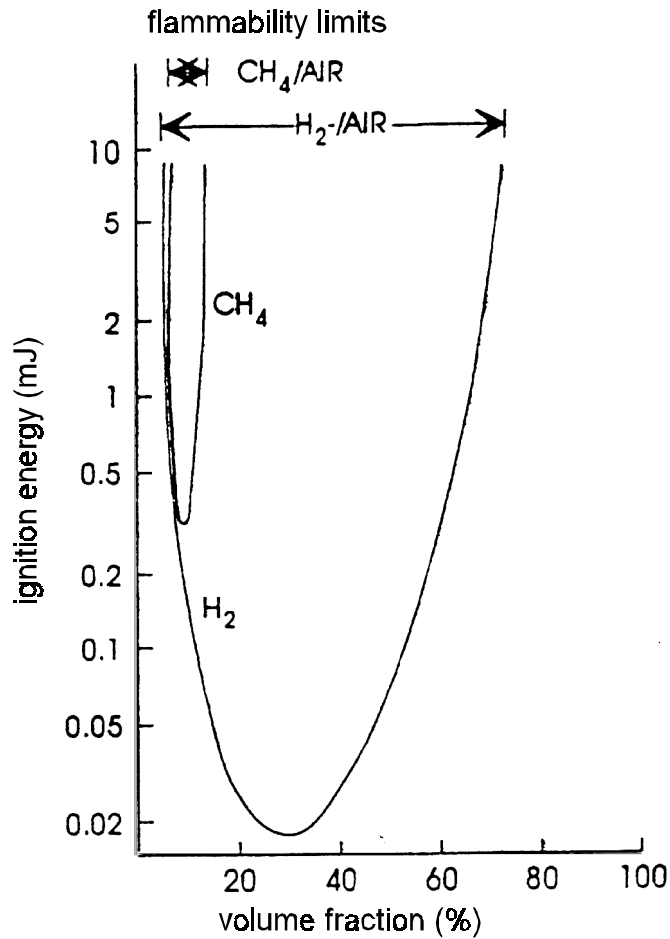
### **3.2.2 Direct hydrogen storage**

An alternative to reformers and chemical hydrides is to store fuel directly in the form of hydrogen. This is easier in terms of system complexity, and the expense of producing the hydrogen is offloaded to central processing plants where hydrogen can be produced from chemical reforming of natural gas or other fossil fuels.

#### *3.2.2.1 Safety*

Hydrogen is often thought of as dangerous fuel. This is partly true; unlike gasoline and most hydrocarbons, which only ignite over a narrow range of fuel-to-air ratios (for example, about 1.3 - 7.1% for gasoline), hydrogen can ignite over a wide range of concentrations (4% - 75% in air).<sup>50</sup> Also, hydrogen has a relatively low ignition energy; a low-energy spark can begin an almost invisible flame (0.2 mJ at stoichiometric conditions in air, less than 10% of the ignition energy of methane, propane, or isooctane.<sup>51</sup>)

Figure 3.7 Ignition energy of hydrogen



Data from Fischer<sup>52</sup>

On the other hand, hydrogen is a very light atom, and leaks tend to disperse quickly. Being lighter than air, hydrogen also tends to diffuse upwards rather than accumulate near the ground. (This benefit could be a problem in indoor situations where the ceiling traps hydrogen). The lower limit of flammability is higher for hydrogen than it is for gasoline, so greater concentrations of hydrogen have to build up before ignition is reached.

Slow leaks in enclosed areas were defined as the greatest risk by a thorough hydrogen safety study done by DTI for Ford and the Department of Energy.<sup>53</sup> Odorants could be added to hydrogen in the same way that they are added to natural gas, except that most sulfur-containing compounds poison platinum catalysts; also, only pure hydrogen can be used in dead-ended systems, because other substances would accumulate in the blocked supply channel.

Scooters in Asia are often driven in a fashion that would be considered reckless in North America. As with gasoline scooters, there is some risk of fire or explosion from a collision; neither gasoline nor hydrogen scooters would be as safe as battery-powered scooters. Safety devices can be designed to shut down power to the battery and cut off hydrogen flow in the case of a collision. Fortunately, the risks are far lower than for automobiles which, due to a combination of their lower fuel economy and greater range, carry about fifteen to twenty times as much fuel. Also, as later modeling will show, fuel cell scooter economy is three or four times that of the equivalent gasoline-powered scooter, so the total energy carried onboard is reduced by 66%-75%.

The following sections describe metal hydride storage and compressed gas cylinders, two forms of easily refillable direct hydrogen storage.

### **3.2.3 Metal hydride energy storage**

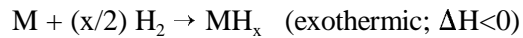
Metal hydrides, which are formed when metal atoms bond with hydrogen to form stable compounds are a good option. Although metals are rather heavy for hydrogen storage, they can uptake a large amount of hydrogen per unit volume so storage density is good. They are typically used as powders in order to maximize the surface area to mass ratio; these metal powders are stored in (low) pressure vessels. Metal hydrides suffer from the problems of high alloy cost,

sensitivity to gaseous impurities, and low gravimetric hydrogen density.

Hydrides have the inherent advantage of being endothermic when releasing hydrogen, increasing safety; in addition, the hydrogen is kept at a relatively low pressure of 1-10 atm within the metal hydride containment cylinder. If the containment vessel is not properly designed, hydrogen embrittlement of the vessel itself is a factor, though, and certain metal hydrides are pyrophoric: they can burn.

### 3.2.3.1 Thermodynamics

The metal hydride adsorption reaction is:



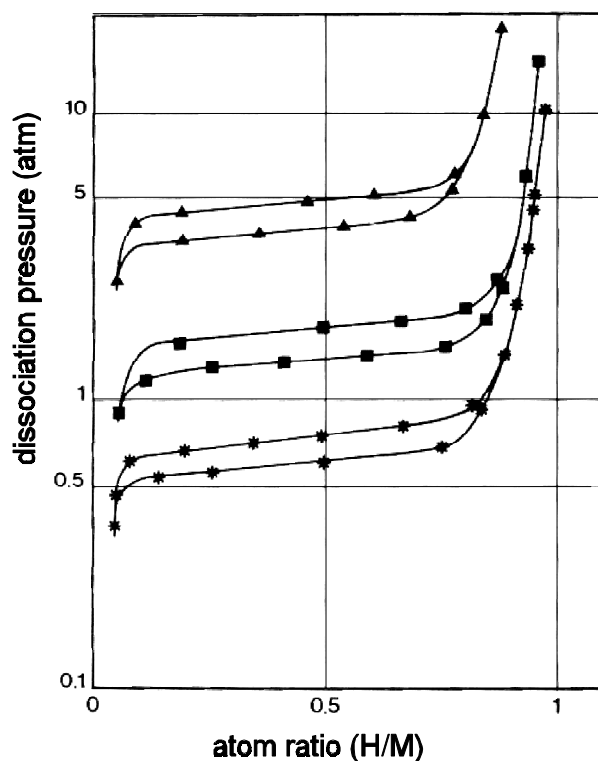
where the number of hydrogen atoms “x” per metal atom “M” is a function of the chemistry of the metal. The exothermicity of the reaction means that more heat causes the equilibrium to shift towards free hydrogen gas, and higher partial pressure of H<sub>2</sub> causes a shift towards adsorption and metal hydride formation. The law of mass action shows that the equilibrium constant is  $K_{eq} = [H_2]^{-(x/2)}$ , and substituting this into the free energy equation illustrates how hydrides are classified.

$$\Delta G = -RT \ln K_{eq} = (x/2) RT \ln (P_{H_2}).$$

A hydride with a high heat of reaction  $\Delta G$  has a lower equilibrium pressure of hydrogen over the metal / metal hydride system at a given temperature, and a stronger metal-hydrogen bond. For a metal to be a useful storage medium for hydrogen, it must easily (strongly) bond to hydrogen so that it can be charged up, but the bond cannot be too strong or else the metal will not give up its hydrogen under depressurization/heating.

Hydrogen uptake shows a characteristic plateaued curve when plotted for isothermal conditions. At low pressures, hydrogen fills the metal structure in interstitial sites as a solid solution. As more hydrogen is injected, the metal begins a phase transition from the  $\alpha$  (metal) phase to the  $\beta$  (metal hydride compound) phase. This is the constant-pressure plateau phase of the isotherm. Above the plateau, the hydrogen concentration can still increase as other compounds begin to form with more hydrogen than the nominal ratio; also, more and more hydrogen molecules compress into the macropores.

Figure 3.8 Metal hydride adsorption curve



Typical metal hydride isotherms for a single metal hydride compound ( $\text{LaNi}_{4.7}\text{Al}_{0.3}$ ) at various temperatures: (\*) at  $30^\circ\text{C}$ , (■) at  $50^\circ\text{C}$ , (▲) at  $80^\circ\text{C}$ . Data from Percheron-Guégan and Welter.<sup>54</sup>

Since the desorption process is endothermic, raising a given hydride to a high temperature at a fixed pressure shifts the equilibrium towards more gaseous  $\text{H}_2$ , while a low temperature means that more gaseous  $\text{H}_2$  is adsorbed. At a constant temperature, the removal of gaseous hydrogen will cause the equilibrium to shift to release more hydrogen from hydride form. This latter situation essentially describes how metal hydrides are used in practice.

Hydrides are also sensitive to contaminants (some are poisoned by oxygen or water vapour) so care must be taken to only introduce pure hydrogen to the hydride.

### 3.2.3.2 Kinetics

The use of metal hydrides as a storage medium for hydrogen is dependent not only on thermodynamics but on kinetics. Fortunately, the intrinsic kinetics of hydrogen dissociation are fast; the rate determining step in general is heat transport into the powder. Powders generally do not conduct heat well, and metal hydride powders are no exception with a thermal conductivity in the range of 1-2  $\text{W}\cdot\text{m}^{-1}\cdot\text{K}^{-1}$ .<sup>55</sup> For comparison, copper, one of the best thermal conductors, has a conductivity of 401  $\text{W}\cdot\text{m}^{-1}\cdot\text{K}^{-1}$ , window glass is at 1.0  $\text{W}\cdot\text{m}^{-1}\cdot\text{K}^{-1}$ ; and fiberglass, a thermal insulator, has a thermal conductivity of 0.05  $\text{W}\cdot\text{m}^{-1}\cdot\text{K}^{-1}$ .<sup>56</sup>

Heat typically needs to be transferred between the walls of the pressure vessel and the powder. While high surface area means fast hydrogen adsorption and desorption, it also means smaller powder particles, which conduct heat more poorly. Schemes thought of to improve conduction include embedding the metal hydride in aluminum foam with high-porosity arteries, or running channels holding hot liquid through the powder. This can increase net thermal conductivity to as much as 7-9  $\text{W}\cdot\text{m}^{-1}\cdot\text{K}^{-1}$ .<sup>57</sup>

Also, hydrogen tends to embrittle the particles and cause them to crack into smaller pieces. This increases the total surface area of the powder, increasing the hydrogen desorption/adsorption rate, but the smaller hydride particles can be entrained in the gas flow, requiring filtering to keep the particles out of the hydrogen output. This leads to concerns about metal hydrides' long term usage.

It might be useful to have some kind of hydrogen storage reservoir between the metal hydride and the fuel cell, in order to damp out peaks and valleys in the hydrogen consumption rate that are lagged by heat transfer into the metal hydride. Fortunately, the gas above the metal hydride in the container can serve this purpose. Transient response time is thus fast, although extended flow rate will depend on the hydrogen desorption rate which in turn is controlled by heat input into the powder.

### 3.2.3.3. Classification

Metal hydrides are classified by the temperature at which the plateau partial pressure of hydrogen ( $H_2$ ) above the metal hydride is greater than 1 atm. The two broad divisions are low-temperature metal hydrides, which have partial pressures of more than 1 bar below  $100^\circ\text{C}$ , and high-temperature metal hydrides, which generally require temperatures of over  $200^\circ\text{C}$  to exceed 1 bar of partial pressure. Some sample specifications are presented below. The data were taken from Browning *et al.*,<sup>58</sup> and a DTI report on hydrogen storage.<sup>59</sup>

**Table 3.7: Theoretical performance of various metal hydrides**

	low-temperature		high-temperature
	$\text{FeTiH}_{1.9}$	$\text{LaNi}_5\text{H}_{6.7}$	$\text{MgH}_2$
<b><math>H_2</math> storage by weight</b>	1.75%	1.43%	7.60%
<b>Density of metal hydride</b>	$5.47 \text{ g}\cdot\text{cm}^{-3}$	$6.59 \text{ g}\cdot\text{cm}^{-3}$	$1.40 \text{ g}\cdot\text{cm}^{-3}$
<b><math>H_2</math> storage by volume</b>	101 g/L	93 g/L	106 g/L
<b>Heat of desorption <math>\Delta H</math> (<math>\text{kJ}\cdot\text{mol } H_2^{-1}</math>)</b>	-28.0	-8.9	-74.0
<b>Dissociation temperature</b>	$50^\circ\text{C}$	$50^\circ\text{C}$	$290^\circ\text{C}$
<b>Desorption pressure at given temp.</b>	10 atm	4 atm	1 atm
<b>DTI estimates of cost</b>	8.80 \$/kg	–	6.60 \$/kg



The chart demonstrates hydrides' excellent volumetric densities but only average weight densities. For vehicle applications, the low temperature hydrides are favoured because the hot exhaust gas from a fuel cell (80°C) can be coupled to the fuel storage system to supply the heat input required for hydrogen evolution; alternately, the fuel cell coolant can be circulated through the metal hydride to dissociate hydrogen from the hydride. High temperature hydrides have perhaps four times the hydrogen weight fractions of low temperature hydrides, but would require the use of burners or other heating devices to reach the 300° needed for 1 atm of hydrogen partial pressure.

For scooters, weight, volume, and safety are the most important concerns. Note that Browning *et al*<sup>9</sup> estimate that the hydride storage container and heat exchange equipment will halve the storage density of metal hydrides; Michael Le of NASA estimates the extra equipment at an extra 50% weight<sup>60</sup>. The latter assumption is used here.

#### 3.2.3.4. *Metal hydride performance*

To compare practically achievable systems, three estimates are made based on existing hydride systems and projections of future performance.

First, Mazda's 20 kW fuel cell electric vehicle, the Demio, runs on an unspecified metal hydride divided into eight modular units. It carries approximately 1.1% hydrogen by weight in the metal hydride (1.4% in the hydride itself, but an extra factor of 1.25 is needed to account for the pressure vessel and attachments), with a volumetric density of 40 g/L. The discharge rate of 0.48 grams per second is enabled by heat transfer from fuel cell cooling water. At 120 MJ/kg LHV for hydrogen, this is a LHV power rate of 57.2 kW, and with an estimated 50% fuel cell efficiency the maximum

*electricity* output rate is 28.5 kW: the quoted 20 kW plus some margin. Total storage is 1.3 kg of hydrogen, for a range of 170 km.<sup>61,62,63,64</sup>

The second estimate is made from characteristics of the metal hydride and cost predictions. If the raw alloy has the storage properties of TiFe as listed in Table 3.7, then to carry 250 grams of hydrogen would require 14.3 kg of hydride and 2.5 L. For raw TiFe alloy, DTI estimates a mass-produced cost of 9 \$/kg<sup>65</sup>, for a total alloy cost of \$100. Assuming that the container and subsystems add 50% to cost, weight, and volume yields final results of 3.7 L, 21.4 kg, and \$190. For “retail” pricing this is doubled to \$380.

For the third comparison, Ergenics offers today a metal hydride hydrogen supply called the ST-90. By default, this system can supply hydrogen at 30 psig at room temperature at a rate of 28 standard liters/minute (0.019 g/s). The system uses “Hy-Stor 208” alloy, with formula  $MmNi_{4.5}Al_{0.5}$  (Mm stands for *mischmetal*, a slightly variable mixture of a number of rare earth elements: approximately, 50% cerium; 32-34% lanthanum; 13-14% neodymium; 4-5% praeodymium; 1.5% other rare earths.<sup>66</sup>) The system is made of stainless steel and is generally sold as one-off units for test and research purposes at a cost of approximately \$10,000.<sup>67</sup> (It should be noted that Ergenics sells the raw Hy-Stor 208 alloy at a cost of 204 \$/kg, accounting for a significant portion of the ST-90 cost.<sup>68</sup> In fact, a Ergenics representative estimated that with a switch from small-scale processing for research purposes to factory manufacturing, costs would be as low as 30 \$/kg.<sup>69</sup>) If designed for custom applications, the transfer rate can be increased to 0.04 g/s by raising the desorption temperature to 45 °C (by a warm water bath, for example), and the weight can be reduced to 27 kg by switching to an aluminum design. Costs on the order of \$3,500-\$4,000 for production in the hundreds is estimated by Ergenics representatives.<sup>70</sup> For true mass production, the costs would drop dramatically, but prediction of costs becomes difficult.

The three predictions are compared below, for predicted system capable of carrying 250 grams of hydrogen and a currently-available hydride system sized at 204 grams.

*Table 3.8 Metal hydride systems comparison*

	<b>Ergenics ST-90 (aluminum)</b>	<b>scaled-down Demio hydride</b>	<b>DTI prediction: scaled-up FeTi</b>
<b>Status</b>	available for sale and use in labs	for vehicle demonstration	projection of future performance
<b>H<sub>2</sub> storage capacity</b>	204 g	250 g	250 g
<b>system weight</b>	27 kg	22.6 kg	21.4 kg
<b>system volume</b>	14 L (2' x 1' x 3")	6.2 L	3.7 L
<b>system H<sub>2</sub> storage by weight</b>	0.76%	1.11%	1.17%
<b>system H<sub>2</sub> storage by volume</b>	15 g/L	40 g/L	67 g/L
<b>cost</b>	\$3,500 (short term)	data not released	\$380 (long term)

Extrapolating the Demio hydride down to 250 grams should not bring up nonlinear scaling issues, since the system is already designed in eight modular containers. The DTI prediction estimates long term cost, while the Ergenics ST-90 represents currently available technology at lab bench scale prices.

Metal hydrides were used in some demonstration fuel cell vehicles but due to their weight and expense are not being considered for the first wave of fuel cell vehicles. On the other hand, small, highly fuel-efficient vehicle like a scooter may be able to take advantage of the safety and low-volume benefits of metal hydrides.

### 3.2.4 Compressed gas storage

One of the less exotic but most practical of the methods of storing hydrogen is to simply compress it as a gas. This increases its density. The major concerns are the large volume required to store the gas even when compressed, and the ability of the container to resist impact.

Storage conditions are set at 3600 psi (standard for natural gas cylinders) at ambient temperature (300° K). 5000 psi cylinders have been suggested for greater storage density, but a more conservative option was chosen here. The Redlich-Kwong equation of state below predicts a molar volume of 0.117 L/mol under these conditions, 16% worse than the 0.101 L/mol calculated by the ideal gas law.

$$\left( P + \frac{a}{V_m (V_m + b) T^{\frac{1}{2}}} \right) (V_m - b) = RT$$

$V_m$  is the volume per mole,  $R$  is the ideal gas constant, and  $P$  is the pressure.  $a$  and  $b$  are empirical constants that can be estimated by the formulas

$$a = 0.42748 \cdot R^2 \cdot T_c^{2.5} / P_c$$

$$b = 0.08664 \cdot R \cdot T_c / P_c$$

where  $T_c$  is the critical temperature,  $P_c$  is the critical pressure, and  $R$  is the ideal gas constant.

The amount of work required to compress the hydrogen gas into the cylinder means that there is an energy penalty of approximately 5-10%. The temperature increases when the hydrogen cylinder is

filled with compressed hydrogen, and the pressure is higher than the nominal operating pressure until the cylinder has a chance to cool; care must be taken not to overpressurize the cylinder. The decrease in temperature during usage due to expansion of hydrogen is not as great a concern, because the release rate is much slower.

Current hydrogen gas storage containers are made from steel alloys that are resistant to hydrogen embrittlement; more advanced cylinders made from aluminum and wrapped with carbon fibre laminate for stiffness are lighter and currently used to contain both natural gas and hydrogen. Less well developed are fully-composite cylinders made solely from carbon fibre impregnated with resin or some other binder; these can have hydrogen gravimetric densities of as much as 9.5% due to their light weight. However, they are more fragile and currently expensive.

#### *3.2.4.1 Cylinder performance*

Dynetek of Calgary currently produces a range of aluminum/carbon cylinders for hydrogen storage. Although the smallest size they manufacture holds 50 L “water volume” (i.e. internal volume), a representative from Dynetek estimated that a cylinder 380 mm long, with 325 mm outside diameter and an internal volume of 20 L could be made. Such a system would weigh 11 kg and have an external volume of 31.5 L. Price would be very dependent on quantities but a Dynetek representative estimated 18-20 \$/L.<sup>70</sup> This system would contain 344 grams of H<sub>2</sub> at the 0.117 L/mol discussed previously. The results are a mass fraction of 3.1%, volumetric density of 10.9 grams H<sub>2</sub>/L<sub>external</sub>, and a cost of \$360. This is a good hydrogen mass fraction, and low-priced for something available today, but poor in terms of volume.

An aerospace-quality gas sphere made by Lincoln Composites weighs 2.4 kg and takes up about

15 L, and holds 8.0 L of internal volume at 3600 psi for a storage density of 5.4 wt%. Two spheres would hold 270 grams of hydrogen at a total weight of 4.8 kg and a volume density of 14.0 g H<sub>2</sub>/L. This is an exceptionally low weight, but 30 L is relatively bulky and fitting two ten-inch spheres in a scooter chassis might be difficult; worse, costs for this aerospace-standard pressure vessel begin at \$5,500 per sphere.<sup>71,72</sup> Where this information is most important is in showing what technical performance is possible.

The smallest natural gas vehicle tank supplied by Lincoln Composites is listed in the table below; it has poorer gravimetric density but is much cheaper at an estimated cost of \$900.<sup>73</sup> Also considered is a pair of carbon composite cylinders from Luxfer Composites.

A final comparison product is an all-metal cylinder. Air Products' size "C" aluminum cylinder weighs 15 kg and holds 15.8 L of internal volume. The cylinder is 84 cm long and 18 cm in diameter (21.4 L external volume) - rather long for a scooter.<sup>74</sup> At its (low) maximum design pressure of 2216 psi, 177 grams of hydrogen can be stored. Hydrogen storage is thus at 1.2 wt% and volumetric density is 8.3 g/L<sub>external</sub>.

The technologies are summarized below. Note that D. Browning *et. al*<sup>75</sup> calculate that pressure regulators add an additional 200 grams to the listed weights.

*Table 3.9 Compressed gas options*

<b>manufacturer</b>	<b>Air Products</b>	<b>Dynetek</b>	<b>Lincoln Composites</b>	<b>Lincoln Composites</b>	<b>Luxfer Composites</b>
<b>model number</b>	“C” model	custom	#220088-1	natural gas 23 L tank	L58C
<b>material</b>	aluminum	carbon w/ aluminum liner	carbon w/ aluminum liner	carbon- polymer	full carbon wrap
<b>storage pressure</b>	2213 psi	3600 psi	3600 psi	3600 psi	3600 psi
<b>radius per unit</b>	9 cm	16 cm	13.1 cm	11.7 cm	7.8 cm
<b>length per unit</b>	84 cm	38 cm	(sphere)	88.9 cm	47.0 cm
<b>external volume</b>	21.4 L	31.5 L	15 L	38.1 L	9.1 L
<b>internal volume</b>	15.8 L	20 L	8.0 L	23.0 L	6.0 L
<b>number of units</b>	1	1	2	1	2
<b>total hydrogen storage</b>	177 g	345 g	280 g	395 g	206 g
<b>total filled weight</b>	15.2 kg	11.3 kg	5.3 kg	17.2 kg	3.7 kg
<b>wt%</b>	1.2%	3.1%	5.5%	2.3%	2.7%
<b>volumetric density (external volume)</b>	8.3 g/L	11.0 g/L	9.4 g/L	10.4 g/L	11.4 g/L
<b>current price per unit</b>	\$250-\$300	\$360	\$5,500	\$900	unknown

In terms of technological feasibility, 5.4% storage is possible, although not practical from a cost perspective. Volumetric densities on the order of 9-12 g/L define the range of possible cylinders, while the Dynetek cylinder is an example of the current commercially available, affordable state-of-the-art. Metal cylinders will likely be too heavy.

#### *3.2.4.2. Cylinder safety*

Natural gas cylinders are typically designed with pressure release devices (PRDs) to discharge the contents of the cylinder in case of fire. Because failure occurs by composite material degradation

rather than by pressure increase, most are eutectic switches designed to release when a certain temperature is reached. The concept of a rapid discharge of hydrogen (under five minutes) is somewhat disturbing, especially considering the fact that these devices are designed to operate when engulfed in flame. On the other hand, a controlled release of flammable hydrogen could very well be better than an abrupt cylinder failure and explosion.

A maximum cylinder lifetime of 15,000 cycles was defined in the standard proposed to the Canadian government by EDO Canada.<sup>76</sup> This would be enough for over 120 years of usage at 45 km per day and one recycle every three days. Thus, the problem of invisible fatigue flaws and microcracks is thus not as much of a concern as abrupt failure due to a collision.

Hydrogen cylinders are likely useful for short term fuel cell scooters, but metal hydrides offer advantages of compact volume and heat removal that are extremely valuable if metal hydride costs can be reduced.

### **3.2.5. Liquid hydrogen storage**

Cryogenic technology and expensive well-insulated cylinders are required if the high volumetric density of liquid hydrogen is to be used. At 20 K and 0.1 MPa vapour pressure, 5.3 wt% H<sub>2</sub> is achievable. Even better, at this temperature liquid hydrogen density is 70 g/L, so carrying 240 grams of hydrogen would only require 3.4 L of liquid hydrogen. However, maintaining the hydrogen at such low temperatures is extremely difficult, with very good insulation, vacuum gaps, and liquid-nitrogen-cooled heat shields typically required. As well, the energy of reducing hydrogen to 20 K and then liquefying it is an important factor when considering liquid hydrogen storage. This energy can amount to an extra 33-40% of the total energy content of the hydrogen.<sup>77</sup>



Another problem is that as heat leaks slowly warm up the liquid hydrogen, more and more is converted into gas over the liquid. Unless this gas is allowed to escape, hydrogen buildup would eventually create leaks in the tank, so a minimum boiloff rate is required and to do this a pressure release valve is needed. A car left unattended for a long period of time would eventually lose all its hydrogen to this safety requirement.

Cryogenic storage for a small scale application like fueling a scooter is not feasible

### **3.2.6 Selection**

The few practical options for storing hydrogen are summarized and considered below. First of all, liquid hydrogen storage is eliminated as being too expensive, difficult to handle, and inefficient for the low storage requirements of scooters, and chemical hydride storage is postponed until future developments demonstrate their practicality. This leaves methanol reforming, metal hydrides, and compressed gas cylinders.

The following table is a comparison of dimensions and weight of storage system required to carry 250 grams of hydrogen. For comparison, a gasoline tank in a scooter is about 5 L, contains approximately 3.7 kg of gasoline, and allows a range of 240 km at 30 km/h, while the battery used in the ZES 2000 scooter is 3.7 L and weighs 38 kg, but only provides 65 km of range at 30 km/h.

*Table 3.10 Storage technology comparison*

	<b>HotSpot reformer + methanol</b>	<b>Dynetek gas cylinder</b>	<b>DTI hydride (includes 50% system factor)</b>
<b>dimensions</b>	–	16 cm radius, 38 cm long cylinder	–
<b>external volume (including tank)</b>	9.4 L	31.5 L	3.7 L
<b>total filled weight</b>	11.1 kg + PROX	11.4 kg	21.4 kg
<b>weight of fuel</b>	1.75 kg CH <sub>3</sub> OH (250 g H <sub>2</sub> )	400 g H <sub>2</sub>	250 g H <sub>2</sub>
<b>wt% of hydrogen in system</b>	< 1.8%	3.6%	1.17%
<b>system volumetric density</b>	22 g/L	12.7 g / L	67 g / L
<b>estimated price</b>	unknown	\$360 (as of 1999)	\$190 (long-term)

Due to their inherent safety, decent hydrogen gravimetric density, and excellent volumetric density, metal hydrides are a good choice for electric scooters. They offer an important side benefit, that of acting as a heat sink for waste fuel cell heat. One difficulty is refueling; since metal hydride tanks are likely to cost over a hundred dollars, swapping fresh packs for old is not likely to be a viable distribution model unless modular units can be made that satisfy a fraction of the refueling need. Refueling at hydrogen pumping stations, an inferior distribution option, is likely necessary but not impossible. On the order of five to fifteen minutes would be required to fill a small metal hydride container, with the fill rate dependent upon pressure and the rate at which the adsorption heat can be removed.<sup>78</sup>

Compressed gas cylinders at 3600 psi are a more well-established technology, but they have the drawbacks of lower safety and poor perception of safety. 31.5 L is likely extremely bulky for a scooter. Refueling would be done from hydrogen filling stations at much higher pressure than for

metal hydrides.

As for reforming, the technology for partial oxidation is well-established, but the final cleanup step required to reduce carbon monoxide from 0.5% to the few ppm required for fuel cell intake is not sufficiently developed to install in a scooter. Reformer technology is quite complex in terms of integrating the various heat and chemical flows, but if hydrogen distribution turns out to be a major stumbling block, reformers would be a fallback option.

## References for Chapter 3

---

1. Supramaniam Srinivasan, personal communication, July 1998
2. Supramaniam Srinivasan, B. B. Davé, K. A. Murugesamoorthi, A. Parthasarathy, and A. J. Appleby "Overview of Fuel Cell Technology". Chapter 2 in *Fuel Cell Systems*, Eds. Leo J. M. J. Blomen and Michael N. Mugerwa. (Plenum Press: 1993), p. 39
3. Supramaniam Srinivasan, personal communication, June 17 1999
4. J. C. Amphlett, M. Farahani, R. F. Mann, B. A. Peppley, P. R. Roberge. "The operation of a solid polymer fuel cell: a parametric model" *Proceedings of the 26th Intersociety Energy Conversion Engineering Conference 1991* (Boston) pp. 624-629
5. Frano Barbir. Energy Partners. "Operating Pressure and Efficiency of Automotive Fuel Cell Systems" No date. 1997 or later.
6. Arvind Parthasarathy *et al.*, p. 103
7. Embrecht Barendrecht, "Electrochemistry of Fuel Cells", Chapter 3 in *Fuel Cell Systems*, Eds. Leo J. M. J. Blomen and Michael N. Mugerwa. (Plenum Press: 1993) p. 94
8. Supramaniam Srinivasan, Fuel Cell Tutorial, August 13 1998.
9. Rioji Anahara. "Phosphoric Acid Fuel Cell Systems", Chapter 8 in *Fuel Cell Systems*, Eds. Leo J. M. J. Blomen and Michael N. Mugerwa. (Plenum Press: 1993) p. 306-307
10. Fritz R. Kalhammer, Paul R. Prokopius, Vernon P. Roan, Gerald E. Voecks. State of California Air Resources Board. *Status and prospects of fuel cells as automobile engines: a report of the fuel cell technical advisory panel*. July 1998. p. III-17
11. *ibid*, p. III-6

12. *ibid*, p. III-17
13. Michael N. Mugerwa and Leo J. M. J. Blomen. "System Design and Optimization", Chapter 6 in *Fuel Cell Systems*, Eds. Leo J. M. J. Blomen and Michael N. Mugerwa. (Plenum Press: 1993) p. 215
14. Hugo Van den Broeck, "Research, Development, and Demonstration of Alkaline Fuel Cell Systems", Chapter 7 in *Fuel Cell Systems*, Eds. Leo J. M. J. Blomen and Michael N. Mugerwa. (Plenum Press: 1993) p. 245
15. Zevco web site. "Zevco News - The Millenium [sic] Taxi" <http://www.zevco.com/news/taxi1.html>. Accessed June 14, 1999
16. Srinivasan Supramaniam, personal communication August 1998
17. S. R. Narayanan, Jet Propulsion Laboratory - Electrochemical Technologies. "Factors Affecting Design and Performance of Direct Methanol Fuel Cell Systems" Presentation at *Fuel Cells for Transportation TOPTEC* March 18-19, 1998 Cambridge, MA
18. *ibid* (Narayanan)
19. Kalhammer, Prokopius, Roan, Voecks. p. II-24
20. *ibid*, p. III-7
21. *ibid*, p. II-24
22. Joan M. Ogden, Margaret Steinbugler, Thomas G. Kreutz. "Hydrogen as a fuel for fuel cell vehicles: a technical and economic comparison" Presentation at National Hydrogen Association 8<sup>th</sup> Annual Conference, Arlington, VA March 11-13, 1997
23. Franklin Lomax, Jr., Brian D. James, George N. Baum, C. E. (Sandy) Thomas. Directed Technologies, Inc. "Detailed Manufacturing Cost Estimates for Polymer Electrolyte Membrane (PEM) Fuel Cells for Light Duty Vehicles". Prepared for The Ford Motor Company under Prime Contract No. DE-AC02-94CE50389 to the U. S. Department of Energy, Office of Transportation Technologies. August 1998, p. 2-2
24. Kalhammer, Prokopius, Roan, Voecks, p. III-23
25. Ballard Power Systems. "Ballard Fuel Cell Stack: Mark 700 Series" product data sheet. August 1998.
26. Peter A. Lehman, Charles E. Chamberlin, Ronald M. Reid, Thomas G. Herron. "Proton Exchange Membrane Fuel Cell". United States Patent number 5,879,826. March 9, 1999
27. Notes of Tom Kreutz from Alfred P. Meyer, International Fuel Cells. "Ambient Pressure PEM Systems" Talk during Fuel Cells for Transportation TOPTEC (SAE), March 18-19, 1998, Cambridge, MA.
28. Peter Lehman *et al.*, U. S. Patent 5,879,826
29. Lisa Fawcett, AMETEK. Personal communication, April 26 1999.
30. D. Picot, R. Metkemeijer, J. J. Beziau, L. Rouveyre. "Impact of the water symmetry factor on humidification and cooling strategies for PEM fuel stacks" in *Journal of Power Sources* **75** (1998) 251-

31. Peter Lehman *et al.*, U. S. Patent 5,879,826
32. Frano Barbir, Energy Partners, Inc. "Operating Pressure and Efficiency of Automotive Fuel Cell Systems"
33. Kalhammer, Prokopius, Roan, Voecks, p. E-3
34. Chris Yang, Princeton University Center for Energy and Environmental Studies, personal communication July 22 1999. The Department of Energy-sponsored research project is operated in conjunction with the Princeton University Chemistry Department.
35. Franklin Lomax Jr., personal communication April 9 1999
36. Ryan Cownden, Meyer Nahon. "Performance Modeling and Improvements of a Solid Polymer Fuel Cell System". Proceedings, The Second International Fuel Cell Conference, February 5-8, 1996. Kobe, Japan.
37. L. E. Unnewehr, S. A. Nasar. *Electric Vehicle Technology*. (John Wiley & Sons, Inc: 1982) p. 52
38. Kalhammer, Prokopius, Roan, Voecks. p. II-11
39. J. H. Hirschenhofer, D. B. Stauffer, R. R. Engleman, M. G. Klett. Parsons Corporation. "Fuel Cell Systems", Chapter 7 of *Fuel Cell Handbook* Fourth Edition. November 1998. p. 7-3
40. Kalhammer, Prokopius, Roan, Voecks. p. II-11
41. Kalhammer, Prokopius, Roan, Voecks p. III-39
42. Neil Edwards, Suzanne R. Ellis, Jonathan C. Frost, Stanislaw E. Golunski, Arjan N. J. van Keulen, Nicklas G. Lindewald, Jessica G. Reinkingh. Johnson Matthey Technology Centre. "On-board hydrogen generation for transport applications: the HotSpot™ methanol processor". *Journal of Power Sources* **71** (Elsevier: 1998) pp. 123-128
43. Joan M. Ogden, Margaret M. Steinbugler, Thomas G. Kreutz. "A comparison of hydrogen, methanol and gasoline as fuels for fuel cell vehicles: implications for vehicle design and infrastructure development" *Journal of Power Sources* **79** (Elsevier: 1999) pp. 143-168
44. R. Metkemeijer, P. Achard "Comparison of Ammonia and Methanol Applied Indirectly in a Hydrogen Fuel Cell" in *International J. Hydrogen Energy* **19** (6) 1994, p. 535
45. Luyu Yang, David P. Bloomfield .Analytic Power Corporation. "Ammonia Cracker for Fuel Cells" *Fuel Cell Seminar 1998 Abstracts*, p. 296
46. Analytic Power web page, "Ammonia Cracker" <http://www.analyticpower.com/NH3CRACK.html>
47. D. Browning, P. Jones, K. Packer. "An investigation of hydrogen storage methods for fuel cell operation with man-portable equipment" *J. Power Sources* **65** (1-2) March-April 1997, pp. 187-195
48. Aldrich. *1998-1999 Catalog Handbook of Fine Chemicals*. LiAlH<sub>4</sub>, p. 1010
49. Alfa Aesar. *Research Chemicals, Metals and Materials 1997-1998*. LiH, p. 317; NaBH<sub>4</sub>, p. 512

50. Ed. Yuda Yurum. *Hydrogen Energy System: production and utilization of hydrogen and future aspects*. Proceedings of the NATO Advanced Study Institute on Hydrogen Energy System, Utilization of Hydrogen and Future Aspects, Akcay, Turkey, August 21 - September 3 1994. (Kluwer: 1994), p. 222
51. Irvin Glassman. Appendix G: Minimum Spark Ignition Energies and Quenching Distances, *Combustion*. Third Edition. (Academic Press: 1996)
52. M. Fischer. "Safety Aspects of Hydrogen Combustion in Hydrogen Energy Systems" *International Journal of Hydrogen Energy* Vol. 11 No. 9, pp. 593-601 quoted in C. E. Thomas, Directed Technologies, Inc. *Direct-Hydrogen Proton-Exchange-Membrane Fuel Cell System for Transportation Applications: Hydrogen Vehicle Safety Report*. Prepared for U. S. Department of Energy, Office of Transportation Technologies. Prepared by Ford Motor Company. May 1997
53. C. E. Thomas. Directed Technologies, Inc. *Direct-Hydrogen Proton-Exchange-Membrane Fuel Cell System for Transportation Applications: Hydrogen Vehicle Safety Report*. Prepared for U. S. Department of Energy, Office of Transportation Technologies. Prepared by Ford Motor Company. May 1997.
54. Annick Percheron-Guégan and Jean-Marie Welter. "Preparation of Intermetallics and Hydrides. Chapter 2 of *Hydrogen in Intermetallic Compounds I: Electronic, Thermodynamic, and Crystallographic Properties, Preparation*. Ed. Louis Schlapbach Topics in Applied Physics Volume 63 (Springer-Verlag, 1988) p. 35
55. G. Sandrock, S. Suda, Louis Schlapbach. "Applications", Chapter 5 in *Topics in Applied Physics Volume 67, Hydrogen in Intermetallic Compounds II: Surface and Dynamic Properties, Applications*. Ed. Louis Schlapbach (Springer-Verlag:: 1992), p. 204
56. David Halliday, Robert Resnick, Jearl Walker. *Fundamentals of Physics*. Fifth Edition. (John Wiley & Sons, Inc. New York: 1997). p. 470
57. Sandrock, Suda, Schlapbach. p. 205
58. Browning, Jones, Packer.
59. Brian D. James, George N. Baum, Franklin D. Lomax, Jr., C. E. (Sandy) Thomas, Ira F. Kuhn, Jr. Directed Technologies, Inc. "Comparison of Onboard Hydrogen Storage for Fuel Cell Vehicles" Task 4.2 Final Report. Prepared for Ford Motor Company under Prime Contract DE-AC02-94CE50389 "Direct Hydrogen Proton-Exchange-Membrane (PEM) Fuel Cell System for Transportation Applications" to the U. S. Department of Energy, pp. 4-56, 4-63, 4-52
60. Michael Le, NASA. Personal communication August 1998
61. Shinichi Hirano, Kenichiro Egusa, Chikara Iname. Technical Research Center (Yokohama), Mazda Motor Corporation. "Development of Electric Vehicle Powered by Polymer Electrolyte Fuel Cell System" Fuel Cell Seminar Abstracts 1998. pp. 730-733
62. Mazda Australia web site. "Mazda" <http://www.mazda.com.au/corpora/460.htm> Accessed June 17, 1999
63. Mazda Japan web page. "Mazda Develops Fuel Cell Electric Vehicle, "Demio FCEV"" <http://www.e.mazda.co.jp/Publicity/Public/9712/971203.html> Accessed June 17, 1999
64. Mazda Japan web page. "From exiting [sic] engines to next generation vehicles" <http://www.e.mazda.co.jp/Action/engine/main3.html> Accessed June 28, 1999

65. James *et al*, p. 4-62
66. Y. Osumi, H. Suzuki, A. Kato, K. Oguro, M. Nakane. *J. Less-Common Met.* **74** (1980) pp. 271-277 in Annick Percheron-Guégan and Jean-Marie Welter, "Preparation of Intermetallics and Hydrides", Chapter 2 in *Topics in Applied Physics Volume 63, Hydrogen in Intermetallic Compounds I: Electronic, Thermodynamic, and Crystallographic Properties, Preparation*. Ed. Louis Schlapbach (Springer-Verlag:: 1988), p. 19
67. Ergenics web site. "ST-90 Metal Hydride Storage Unit" <http://www.ergenics.com/st90.htm> Accessed July 1, 1999
68. Ergenics web site. "Price List" <http://www.ergenics.com/alloyPL.htm> Accessed July 1, 1999
69. Dave Tragna, Ergenics. Personal communication, March 3 1999
70. Colin Armstrong, Dynetek. personal communication, October 5 1998
71. Lincoln Composites web page. "Pressure Vessels for Aircraft and Missile Applications" [http://www.lincolncomposites.com/products/pv\\_details/space.html](http://www.lincolncomposites.com/products/pv_details/space.html). Accessed June 1, 1999
72. Jack Schimenti, Aerospace/Defense business manager. Lincoln Composites. Personal communication June 1, 1999
73. Christine Simentich, Natural Gas Vehicle Tanks. Lincoln Composites. Personal communication June 1, 1999
74. Air Products web site, "Specialty Gas Cylinder Information" <http://www.airproducts.com/specgas/cylind/cylind.htm>
75. Browning, Jones, Packer.
76. EDO Canada Limited. *Compressed Hydrogen gas vehicle cylinder development* Transport Canada document TP 13023E. April 1997
77. Joan Ogden, Princeton University. Personal communication July 22 1999
78. *ibid.*